

56p

N63-12927
code-1



TECHNICAL NOTE

D-1501

AN APPLICATION OF A
NUMERICAL TECHNIQUE TO LIFTING-SURFACE THEORY
FOR CALCULATION OF UNSTEADY AERODYNAMIC FORCES DUE TO
CONTINUOUS SINUSOIDAL GUSTS ON SEVERAL WING PLANFORMS
AT SUBSONIC SPEEDS

By Harold N. Murrow, Kermit G. Pratt,
and Joseph A. Drischler

Langley Research Center
Langley Station, Hampton, Va.

NATIONAL AERONAUTICS AND SPACE ADMINISTRATION
WASHINGTON

February 1963

Code 1

Copy 1

NATIONAL AERONAUTICS AND SPACE ADMINISTRATION

TECHNICAL NOTE D-1501

AN APPLICATION OF A
NUMERICAL TECHNIQUE TO LIFTING-SURFACE THEORY
FOR CALCULATION OF UNSTEADY AERODYNAMIC FORCES DUE TO
CONTINUOUS SINUSOIDAL GUSTS ON SEVERAL WING PLANFORMS
AT SUBSONIC SPEEDS

By Harold N. Murrow, Kermit G. Pratt,
and Joseph A. Drischler

SUMMARY

A numerical lifting-surface method has been used to calculate direct gust forces and moments on wings of several planforms. The gust velocities are continuous and vary sinusoidally in the stream direction and are also uniform across the wing span. The procedure has the advantage of rapid machine calculation and includes the effects of wing planform, nonsteady subsonic flow, and induced flow effects. The method provides for calculation of gust forces on a basis consistent with that for the calculation of forces due to motion and deformation. The results include the in-phase and quadrature components of the following quantities: (a) spanwise distribution of section lift coefficient, (b) total lift coefficient, and (c) total pitching-moment coefficient. In addition, generalized gust forces on approximate fundamental cantilever bending modes (parabolic) are also included. Results have been obtained for 60° and 75° delta wings, 35° sweptback wings of aspect ratio 4.00 and 9.43, a 5° sweptback wing of aspect ratio 11.60, and an unswept wing of aspect ratio 6.00. Conditions for which calculations were made include two Mach numbers (generally, 0.40 and 0.90) and a reduced-frequency range of 0 to 1.0. The direct gust forces and moments are in forms suitable to be inserted in equations of motion used in the calculation of the dynamic responses of flexible lifting vehicles to random turbulence and to be compared with results from other methods.

INTRODUCTION

Current analytic methods for calculating airplane responses to continuous vertical atmospheric turbulence (random process theory) require a knowledge of unsteady generalized aerodynamic forces due directly to turbulence velocities. Within the framework of random process theory, these aerodynamic forces are described in terms of the forces produced directly by vertical gust velocities

which vary sinusoidally along the flight path of the airplane and which are uniform along the span of the lifting surface. For convenience in application, values of unsteady aerodynamic forces due to these inputs are desired for the planform of interest.

Explicit solutions of the aerodynamic equations for a general lifting surface have not been found. Approximations involving strip theory have been utilized, such as the use of steady-state spanwise lift distributions together with an amplitude function based on two-dimensional flow and simple time lags to account for gust field penetration. Results of work on unsteady aerodynamic forces pertinent to gust analysis can be found in references 1 to 4. Information for wings of finite aspect ratio in subsonic compressible flow is very limited.

Reference 5 has provided a numerical method for solving the equations for a lifting surface (utilizing a high-speed digital computer) which can be used for calculating sinusoidal gust forces in subsonic flow. This method was developed primarily for flutter studies, but the applied downwash description permits it to be extended to the gust case. It therefore provides aerodynamic forces on a consistent basis for both oscillating airstream and oscillating lifting surfaces. An application of this technique to a swept wing has been demonstrated as an incidental part of the study of reference 6 with satisfactory results indicated.

The purpose of the present report is (1) to demonstrate the application of the procedure of reference 5 to the calculation of generalized forces, including lift and pitching moments, due to sinusoidal gusts for several commonly used wing planforms and (2) to present these results in the form of curves that may be utilized in simplified calculations. The data for planforms considered herein include results at two subsonic Mach numbers for 60° and 75° delta wings, 35° sweptback wings of two aspect ratios, one 5° sweptback wing, and two unswept wings. A comparison is made of the results of the numerical procedure and those of a modified strip theory. These results will add to the limited available information on unsteady lift functions for some typical wings of finite aspect ratio in sinusoidal gusts in subsonic flow.

SYMBOLS

A	aspect ratio, b^2/S
A_1, B_1	real and imaginary parts, respectively, of spanwise distribution of generalized gust force per unit gust velocity
A_1^*, B_1^*	normalized values of A_1 and B_1 , respectively (see section entitled "Gust Forces")
b	wing span, ft
C_1, D_1	real and imaginary parts, respectively, of total generalized gust force

C_i^*, D_i^*	normalized values of C_i and D_i , respectively (see section entitled "Gust Forces")
C_L	lift coefficient, L/qS
C_m	pitching-moment coefficient, $2M_Y/qSc_r$
$C_{L\alpha}$	lift-curve slope, $dC_L/d\alpha$, per radian
c	local wing chord, ft
c_a	average chord, S/b , ft
c_l	section lift coefficient
c_r	root chord of lifting surface, ft
c_t	wing chord at tip, ft
K	kernel of equation (2), integral equation (see ref. 5)
k	reduced-frequency parameter, $\omega c_r/2U$
L	lift-force, lb
M	Mach number
M_{ij}	generalized inertia force or moment coefficient representing coupling between i th and j th modes, slugs
M_Y	pitching moment about midpoint of root chord, positive nose up
P, Q	real and imaginary parts, respectively, of normalized unsteady lift function for wing of infinite aspect ratio; for steady flow: $P = 1$, $Q = 0$
Δp	differential pressure, lb/sq ft
Δp_j^M	pressure distribution due to downwash of j th mode, per unit generalized coordinate, $\partial \Delta p^M / \partial q_j$
$\frac{\Delta p^G}{\bar{w}_g}$	pressure distribution due to gust downwash, per unit downwash velocity
$Q_i(\omega)$	i th mode generalized aerodynamic force or moment
Q_i^G	generalized aerodynamic force due to unit gust velocity

$Q_{ij}^M(\omega)$ generalized aerodynamic force due to wing motion
 q dynamic pressure, $\rho U^2/2$, lb/sq ft
 $q_i(\omega), q_j(\omega)$ ith and jth generalized coordinates, respectively
 S wing area, sq ft
 t time, sec
 U velocity of airstream, ft/sec
 w applied downwash velocity, ft/sec
 w_g gust downwash velocity, ft/sec
 x coordinate along chord of lifting surface measured rearward from
 leading edge of root chord
 y coordinate along semispan of lifting surface measured outward from
 root chord
 $y^* = \frac{y}{b/2}$
 z wing deflection, ft
 α angle of attack, radians
 Λ sweepback angle of 1/4 chord line of lifting surface, deg
 Λ_{le} sweepback angle of leading edge of lifting surface, deg
 λ wavelength, ft/cycle
 λ_T taper ratio, c_t/c_r
 $\xi_i(x,y)$ shape of ith mode of airplane structure
 ρ density of air, slugs/cu ft
 ω frequency, radians/sec

Subscripts:

i, j integers indicating modes

A bar above a symbol indicates amplitude only.

ANALYSIS

In this section the relationship of the gust force terms to the other terms in the general equations of motion will be shown. The numerical procedure for determining the pressure distribution over the lifting surface will also be briefly described.

Gust Forces

The general equations of motion based on uncoupled modes of motion and deformation for an airplane flying through a continuous sinusoidal gust field can be written as follows (based on refs. 6 and 7):

$$-\omega^2 \sum_{j=1}^n M_{ij} q_j(\omega) + \omega_i^2 M_{ii}(\omega) q_i(\omega) = Q_i(\omega) = \sum_{j=1}^n Q_{ij}^M(\omega) q_j(\omega) + Q_i^G(\omega) \bar{w}_g \quad (i = 1, 2, 3, \dots n) \quad (1a)$$

where the terms $Q_{ij}^M(\omega)$ and $Q_i^G(\omega)$ are the generalized aerodynamic forces due to airplane motion and gust velocity, respectively. The generalized forces on the right-hand side of the equation are defined as

$$Q_{ij}^M(\omega) = \iint_S \xi_i(x,y) \frac{\partial \Delta p^M}{\partial q_j}(x,y;\omega) dx dy \quad (1b)$$

and

$$Q_i^G(\omega) = \iint_S \xi_i(x,y) \frac{\Delta p^G}{\bar{w}_g}(x,y;\omega) dx dy \quad (1c)$$

This report is concerned with the determination of generalized gust forces $Q_i^G(\omega)$. Integrating equation (1c) over the chord yields

$$Q_i^G(\omega) = \int_0^1 \left[A_i(y^*, \omega) + iB_i(y^*, \omega) \right] dy^* \quad (1d)$$

where A_i and B_i represent the real and imaginary parts, respectively, of the spanwise distribution of the generalized gust forces per unit amplitude of gust velocity. The terminology used herein of real and imaginary implies the in-phase

and out-of-phase components of a quantity with respect to the applied downwash at the leading edge of the root chord of the lifting surface. Integrating equation (1d) over the span yields

$$Q_i^G(\omega) = C_i(\omega) + iD_i(\omega) \quad (1e)$$

where C_i and D_i represent the real and imaginary parts, respectively, of the total generalized gust forces.

For many applications the degrees of freedom of rigid-body translation, rigid-body pitch, and first flexible bending mode of vibration are sufficient to determine the desired result. Consequently, the results presented herein are responses for these degrees of freedom. These results are as follows, referring to equation (1c):

(1) For rigid-body translation, $i = 1$ and $\xi_1 = 1$; therefore, A_1 and B_1 may be interpreted as the real and imaginary parts of the spanwise lift distribution. The terms C_1 and D_1 are then the real and imaginary parts of the total lift obtained by integrating A_1 and B_1 over the span of the lifting surface. For purposes of emphasizing the nonsteady flow characteristics, normalized values of C_1 and D_1 are obtained from integration after dividing A_1 and B_1 by the modulus of the steady-state lift $\sqrt{C_1^2 + D_1^2}$. These normalized values will be designated C_1^* and D_1^* .

(2) For purposes of presentation, the quantities A_1 and B_1 have been normalized by dividing each value of A_1 and B_1 by the magnitude of the total lift for the frequency under consideration. This procedure eliminates the effect of magnitude and illustrates the effect of reduced frequency on the in-phase and quadrature portions of the spanwise lift distribution. These normalized values will be designated A_1^* and B_1^* .

(3) For rigid-body pitch, $i = 2$ and $\xi_2 = x$; thus, C_2 and D_2 may be interpreted as the real and imaginary parts of the total pitching moment. As was the case for C_1 and D_1 , C_2 and D_2 will be presented as normalized values C_2^* and D_2^* . These are obtained by dividing A_2 and B_2 by the modulus of the steady-state moment $\sqrt{C_2^2 + D_2^2}$.

(4) For a first bending mode approximated by a parabolic spanwise shape, $i = 3$ and $\xi_3 = (y^*)^2$. Since ξ_3 is only a function of y , $A_3 = A_1(y^*)^2$ and $B_3 = B_1(y^*)^2$. Spanwise integration yields C_3 and D_3 which are the real and imaginary parts of the gust forces for this mode shape.

In this paper A_1^* and B_1^* , C_1^* and D_1^* , C_2^* and D_2^* , and C_3/qS and D_3/qS will subsequently be presented for the various planforms considered.

Determination of Pressure Distribution

The real and imaginary components of the pressure distribution $\Delta p^G/\bar{w}_g$ in equation (1c) are obtained by the numerical method of reference 5 with the substitution of an expression for the gust downwash for that of motion and deformation downwash. A brief description of some of the features of the numerical method and of the expression for the gust downwash is given below.

The numerical method is applied to the solution of a linear integral equation of the form

$$w(x,y) = \frac{U}{8\pi q} \iint_S \Delta p(\xi, \eta) K(x-\xi, y-\eta; k, M) d\xi d\eta \quad (2)$$

The function K , the kernel of the integral equation, physically represents the contribution to the downwash at a field point (x,y) due to a sinusoidally pulsating pressure doublet of unit strength located at any point (ξ, η) . The solution of the equation is obtained from a high-speed digital computer program which requires only that the following information be provided:

- (1) The coordinates of nine¹ control points on one-half of the wing and the downwash at each point
- (2) The parameters that describe the wing boundaries
- (3) The subsonic Mach number
- (4) The values of the reduced frequency $k = \omega c_r/2U$ for which solutions are desired

The method of reference 5 was developed for flutter studies; consequently, the expression given therein for the downwash is in terms of sinusoidal wing motion and deformation. This expression can be written

$$w(x,y)e^{i\omega t} = \left[U \frac{\partial z}{\partial x}(x,y) + i\omega z(x,y) \right] e^{i\omega t} \quad (3)$$

For the generalized gust forces no motion or deformation of the wing is desired in the expression for the downwash. Rather, the downwash expression must account for the sinusoidal variation of the gust downwash along the wing in the chordwise direction. The appropriate expression is

¹Since preparation of this report, the computer program has been extended to 12 and 16 control points.

$$w(x,y)e^{i\omega t} = w_g e^{i\omega t} = \bar{w}_g e^{i\omega\left(t - \frac{x_c}{U}\right)} \quad (4)$$

where x_c is the location of a control station relative to the leading edge of the root chord. Equation (4) can be written

$$w(x,y)e^{i\omega t} = \bar{w}_g e^{i\omega t} \left(\cos 2k \frac{x_c}{c_r} - i \sin 2k \frac{x_c}{c_r} \right) \quad (5)$$

where

$$k = \frac{\omega c_r}{2U}$$

For this downwash the pressure distributions are obtained numerically and the generalized gust force is obtained by integrating over the lifting surface. (See ref. 5.)

RESULTS AND DISCUSSION

Presentation of Results

The planforms for which results are presented herein are shown in figure 1. These planforms include 60° and 75° delta wings and two wings with quarter-chord sweepback angle of 35° and taper ratio of 0.42, with aspect ratios of 9.43 and 4.00. Also included is a wing with a 5° sweepback angle, aspect ratio of 11.60, and taper ratio of 0.44. Unswept wings are also considered; the results for the "classic" rectangular wing of aspect ratio 6.00 are included for comparison along with an unswept wing (quarter-chord line perpendicular to root chord) of aspect ratio 6.00 and taper ratio 0.50.

Calculated values of steady-state lift- and pitching-moment-curve slopes for all planforms considered are shown in table I. Some of these values are discussed in a subsequent section entitled "Limitations."

Values of the normalized real and imaginary parts of the generalized gust force for vertical translation (total lift), C_1^* and D_1^* , respectively, are given in figures 2(a) to 2(h). The phase relationship is given with respect to the downwash at the leading edge of the root chord. Figure 2(a) gives results from reference 1 (generally termed P and Q) which are for a wing with infinite aspect ratio in incompressible flow ($M = 0$) and provides a convenient reference for the results for all the other planforms. Figure 2(b) gives results for a rectangular wing of aspect ratio 6.00 in incompressible flow. A comparison of present results with those obtained by using the approximation given in equation (33) of reference 4 is shown in figure 2(b) and shows almost the same results.

Values of the normalized real and imaginary parts of the generalized gust force for rigid pitching motion (total pitching moment) are given in figures 3(a) to 3(f) as C_2^* and D_2^* . This pitching moment is about the midpoint of the root chord of the lifting surface. The moment relation used is $M_Y = C_m q S \frac{c_r}{2}$.

The normalized real and imaginary parts of the spanwise distribution of generalized gust forces for rigid-body translation (lift) A_1^* and B_1^* are shown in figures 4(a) to 4(m) for the various planforms at two Mach numbers and various values of k (generally 0, 0.5, and 1.0). It should be noted again that all phase relationships are with respect to the downwash at the leading edge of the root chord of each planform. All curves presented would, of course, exhibit significant changes if the downwash reference were shifted to another location.

Figures 5(a) to 5(g) present values for the real and imaginary parts of the generalized gust-force coefficients for a deflection mode with a parabolic shape approximating the first wing bending mode C_3/qS and D_3/qS .

Discussion

Limitations.- The present procedure provides for the calculation of generalized gust forces on a basis consistent with that for the calculation of generalized aerodynamic forces due to motion and deformation of a lifting surface. It is the purpose of this section to indicate the range of configurations and conditions for which the preceding statement applies. The principal limitations are with respect to aspect ratio and reduced frequency with a slight limitation on the subsonic Mach number range, the maximum Mach number being approximately 0.95.

The application of the present procedure is limited to the lower values of aspect ratio - say to less than 10 or 12. In general, errors increase with an increase in aspect ratio. This error as displayed by the steady-state lift-curve slope for a rectangular wing in incompressible flow ($M = 0$) is illustrated in the following table. Values calculated by the present procedure are given in the second column. Particularly noteworthy is the value for aspect ratio 20 of more than 2π (the limit value for infinite aspect ratio).

Aspect ratio	Steady-state lift-curve slope obtained from -		
	Present method	Lifting-line theory (ref. 8)	Lifting-surface theory (ref. 9)
6	4.28	4.18	4.30
10	5.34	^a 4.81	----
12	^a 5.68	5.00	----
15	6.15	-----	----
20	6.84	-----	----

^aInterpolated values.

A further indication of the error in the present procedure is provided by a comparison of the results with those from steady-state lifting-line theory presented in the third column. The latter results were obtained from information in reference 8 and are considered to be progressively more accurate with increasing aspect ratio. In contrast, the results of the present numerical procedure become more accurate with decreasing aspect ratio. The tabulation indicates that errors in the results of the present procedure are less than about 10 percent for aspect ratios less than 10. The source of the errors at the higher aspect ratios is thought to be the limited number of control points and the particular numerical integration employed.

An additional assessment of the present procedure may be made from the preceding tabulation. The lift-curve slope for an aspect ratio of 6, obtained from lifting-surface equations by a different method of solution described in reference 9, is given in the fourth column. The close agreement with results from the present method indicates consistency of results from applying lifting-surface theories at the lower aspect ratios.

Inasmuch as the aspect ratios of two of the several wing configurations considered herein were in the vicinity of 10, the errors with respect to the results of lifting-line theory were investigated in a manner similar to that for the rectangular wing. The data from lifting-line theory were obtained by interpolation of results from references 8 and 10. Prandtl-Glauert corrections for compressible flow were made in accordance with the procedure described in reference 10. The results are presented in the following table:

Planform	A	λ_T	M	Steady-state lift-curve slope obtained from -	
				Present method	References 8 and 10
5° swept	11.60	0.44	0.33	6.08	5.36
5° swept	11.60	.44	.70	7.55	6.65
35° swept	9.43	.42	.58	5.06	4.66
35° swept	9.43	.42	.90	6.32	5.85

The variations of error with aspect ratio are consistent with those for the rectangular wing.

There is a value of reduced frequency beyond which errors in the present procedure become excessive. This limitation arises because, in the present usage, the applied downwash is satisfied at only three points along the chord, at each of three semispan stations. In numerical operations it is common practice to require at least nine or ten uniformly spaced points to describe a cycle of a sine function. Therefore, in the present procedure, errors may be expected to increase sharply for frequencies greater than those having a wavelength of about 3 chords. For all wings considered herein, the maximum chord is the root chord and the frequency limitation can be expressed as

$$\lambda > 3c_r \quad (6a)$$

and

$$\lambda = \frac{2\pi U}{\omega} = \frac{\pi c_r}{k_1} \quad (6b)$$

Therefore,

$$\frac{\pi c_r}{k_1} > 3c_r \quad (6c)$$

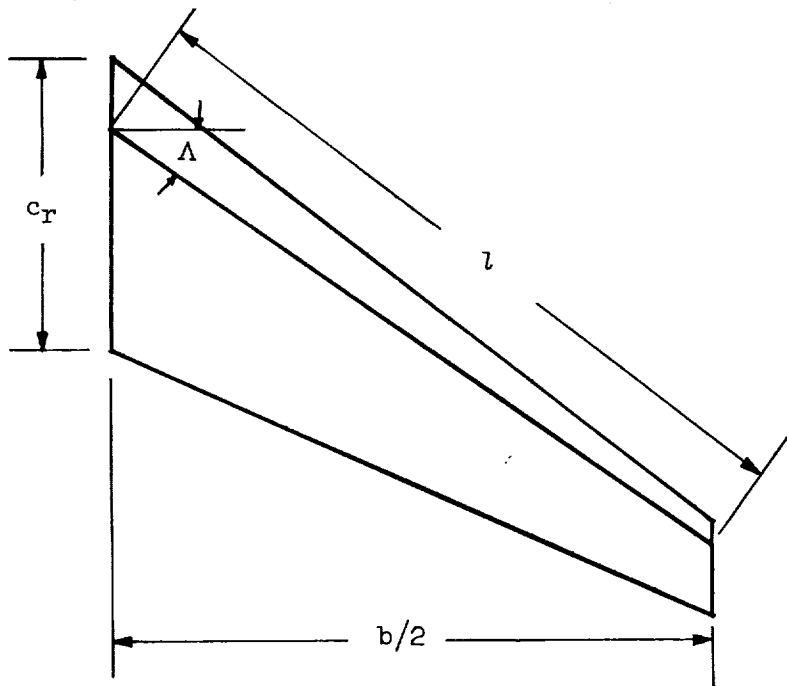
and

$$k_1 < \frac{\pi}{3} \quad (6d)$$

or approximately,

$$k_1 < 1 \quad (6e)$$

A similar limit in reduced frequency arises for sweptback wings due to a sinusoidal variation of downwash along a line through the most forward control points (in this case, the quarter-chord line) of the wing and replaces the limit described previously for the condition $\frac{c_r}{b/2} < \tan \Lambda$ as will be indicated. The following sketch is presented to clarify the terminology.



To approximate a sinusoid along the span

$$\lambda = \frac{\pi c_r}{k_2} > 3l \sin \Lambda \quad (7a)$$

but

$$l = \frac{b/2}{\cos \Lambda} = \text{Wing length along quarter-chord line} \quad (7b)$$

hence,

$$k_2 < \frac{\pi}{3} \frac{c_r}{\frac{b}{2} \tan \Lambda} \quad (7c)$$

For the limitation of equation (7c) to apply,

$$k_2 < k_1$$

and, for this condition, considering equations (6d) and 7(c),

$$\frac{\pi}{3} \frac{c_r}{\frac{b}{2} \tan \Lambda} < \frac{\pi}{3} \quad (7d)$$

therefore,

$$\frac{c_r}{b/2} < \tan \Lambda \quad (7e)$$

For example, for $\Lambda = 35^\circ$ and $\frac{b/2}{c_r} = 3.35$, it can be seen that $\frac{1}{3.35} < 0.700$;

therefore, k_2 is the limiting reduced frequency and $k_2 < \frac{\pi}{3} \frac{1}{3.35(0.700)}$ or $k_2 < 0.446$. Thus, for this planform the limitation on k_2 due to sweep is quite severe. For numerical procedures using more control points, limitations on k_1 or k_2 may be relaxed.

Application of tables and figures.- As mentioned previously, some of the results were normalized to illustrate better the effects of nonsteady flow in terms of reduced frequency. For application to airplane-response calculations, these results must be converted to forces, as defined by equation (1d), suitable for insertion into equation (1). The necessary conversions are described in the following paragraphs.

The results in figures 2 and 3 are converted by use of the equations

$$Q_1^G = C_1(k) + iD_1(k) = \left(\frac{dC_L}{d\alpha} \right)_{k=0} qS [C_1^*(k) + iD_1^*(k)] \quad (8)$$

and

$$Q_2^G = C_2(k) + iD_2(k) = \left(\frac{dC_m}{d\alpha} \right)_{k=0} \frac{qSc_r}{2} [C_2^*(k) + iD_2^*(k)] \quad (9)$$

respectively.

The results in figure 4 are converted to spanwise force distributions suitable for computing generalized gust forces on flexible wing bending modes by use of the equation

$$A_1(y^*, k) + iB_1(y^*, k) = qS \left(\frac{dC_L}{d\alpha} \right)_{k=0} \sqrt{[C_1^*(k)]^2 + [D_1^*(k)]^2} [A_1^*(y^*, k) + iB_1^*(y^*, k)] \quad (10)$$

The results in figure 5 may be converted to generalized gust forces on parabolic wing bending modes by multiplication by qS .

The values of $\left(\frac{dC_L}{d\alpha} \right)_{k=0}$ and $\left(\frac{dC_m}{d\alpha} \right)_{k=0}$ used in equations (8) to (10) are given in table I.

Comparisons with modified strip theory.- In the absence of a procedure or the facilities for a rapid numerical solution of lifting-surface equations, there is a temptation to consider some form of strip theory. In this section a comparison is made of results of a strip theory with those of the numerical lifting-surface calculations.

One form of strip theory which appears to offer a useful approximation for gust-force calculations for wings of moderate to large aspect ratio consists of assuming that the lift at a local point on the span is equal to the lift at that

point based on the steady-state lift distribution $\left(\frac{c_l c}{C_L c_a} \right)_{\alpha=\text{Constant}}$ for the

three-dimensional surface in a uniform downwash (see refs. 8 and 10) multiplied by the local angle of attack at the leading edge w_{le}/U and by the nonsteady lift function for a wing of infinite aspect ratio in a sinusoidal gust field $P + iQ$ (see ref. 1, for example).

This may be expressed as

$$\left(\frac{c_l c}{C_L c_a}\right) \frac{\bar{w}_g}{U} e^{i\omega t} = \left(\frac{c_l c}{C_L c_a}\right)_{\alpha=\text{Constant}} \frac{w_{le}}{U} \left[P\left(\frac{k c}{c_r}\right) + iQ\left(\frac{k c}{c_r}\right) \right] \quad (11)$$

where

$$w_{le} = \bar{w}_g e^{i\omega \left(t - \frac{y \tan \Lambda_{le}}{U} \right)}$$

and describes the lag of penetration of the leading edge at the local chord relative to the leading edge at the root chord.

This equation is related to the generalized gust force, Q_1^G , for example, by

$$Q_1^G = \frac{q S C_{L\alpha}}{U} \int_0^1 \frac{c_l c}{C_L c_a} dy^*$$

or

$$Q_1^G = \frac{q S C_{L\alpha}}{U} \int_0^1 \left(\frac{c_l c}{C_L c_a}\right)_{\alpha=\text{Constant}} \left[P\left(\frac{k c}{c_r}\right) + iQ\left(\frac{k c}{c_r}\right) \right] \left[\cos\left(\frac{\omega y}{U} \tan \Lambda_{le}\right) - i \sin\left(\frac{\omega y}{U} \tan \Lambda_{le}\right) \right] dy^* \quad (12)$$

from which

$$A_1^*(y^*, k) = \left[P\left(\frac{k c}{c_r}\right) \cos\left(\frac{k b y^*}{c_r} \tan \Lambda_{le}\right) + Q\left(\frac{k c}{c_r}\right) \sin\left(\frac{k b y^*}{c_r} \tan \Lambda_{le}\right) \right] \left(\frac{c_l c}{C_L c_a}\right)_{\alpha=\text{Constant}} \frac{\bar{Q}_1^G(k=0)}{\bar{Q}_1^G(k)} \quad (13)$$

and

$$B_1^*(y^*, k) = \left[Q\left(\frac{k c}{c_r}\right) \cos\left(\frac{k b y^*}{c_r} \tan \Lambda_{le}\right) - P\left(\frac{k c}{c_r}\right) \sin\left(\frac{k b y^*}{c_r} \tan \Lambda_{le}\right) \right] \left(\frac{c_l c}{C_L c_a}\right)_{\alpha=\text{Constant}} \frac{\bar{Q}_1^G(k=0)}{\bar{Q}_1^G(k)} \quad (14)$$

where

$$y^* = \frac{y}{b/2}$$

and

$$\frac{c}{c_r} = 1 - (1 - \lambda_T)y^* \quad (15)$$

For purposes of comparison with the results of the numerical lifting-surface calculations, A_1^* and B_1^* from the strip theory were calculated for a 35° sweptback wing and for a 60° delta wing. The Prandtl-Glauert compressibility correction as described in reference 10 was applied and the nearest geometric configuration of sweep, taper ratio, and aspect ratio was used to obtain

$\left(\frac{c_{l^c}}{C_{L^c a}}\right)_{\alpha=\text{Constant}}$ from reference 8. The function $P(k) + iQ(k)$ was obtained

from results given in reference 1. As indicated in equation (12), in the application the reduced frequency k was based on the local chord. A check has shown very little difference between these results and those for $P(k) + iQ(k)$ with the reduced frequency based on the root chord.

The results of the strip theory in the form of A_1^* and B_1^* are given, together with those of the numerical lifting-surface calculations, in figures 6(a) and 6(b) for the 35° sweptback wing and in figure 6(c) for the 60° delta wing. The two sets of results agree fairly well for both wings at the frequencies considered and should compare similarly for other frequencies lower than the highest shown. Although not presented in the figures, values of C_1^* and D_1^* from strip theory are generally somewhat lower than those from the lifting-surface calculations. The ratios of amplitudes are about 78 percent for the rectangular wing with $A = 6.00$; 88 percent for the 35° swept wing with $A = 9.43$; and 85 percent for the 60° delta wing.

CONCLUDING REMARKS

The responses of six wing planforms to continuous sinusoidal gusts have been calculated by the use of a lifting-surface procedure. This procedure provides for the calculation of generalized gust forces on a basis consistent with that for the calculation of generalized aerodynamic forces due to motion and deformation of a lifting surface. There are known limitations to the procedure, however, and these are discussed; the procedure is limited to aspect ratios less than about 10. The gust forces and moments are in forms suitable to be inserted in equations of motion for calculation of dynamic responses of lifting surfaces to random turbulence.

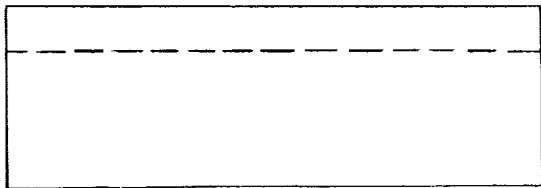
Langley Research Center,
National Aeronautics and Space Administration,
Langley Station, Hampton, Va., August 20, 1962.

REFERENCES

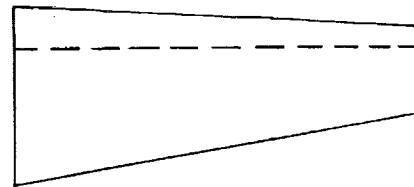
1. Sears, William R.: Some Aspects of Non-Stationary Airfoil Theory and Its Practical Application. Jour. Aero. Sci., vol. 8, no. 3, Jan. 1941, pp. 104-108.
2. Jones, Robert T.: The Unsteady Lift of a Wing of Finite Aspect Ratio. NACA Rep. 681, 1940.
3. Garrick, I. E.: On Some Fourier Transforms in the Theory of Non-Stationary Flows. Proc. Fifth Int. Cong. Appl. Mech. (Cambridge, Mass., 1938), John Wiley & Sons, Inc., 1939, pp. 590-593.
4. Drischler, Joseph A.: Calculation and Compilation of the Unsteady-Lift Functions for a Rigid Wing Subjected to Sinusoidal Gusts and to Sinusoidal Sinking Oscillations. NACA TN 3748, 1956.
5. Watkins, Charles E., Woolston, Donald S., and Cunningham, Herbert J.: A Systematic Kernel Function Procedure for Determining Aerodynamic Forces on Oscillating or Steady Finite Wings at Subsonic Speeds. NASA TR R-48, 1959.
6. Bennett, Floyd V., and Pratt, Kermit G.: Calculated Responses of a Large Sweptwing Airplane to Continuous Turbulence With Flight-Test Comparisons. NASA TR R-69, 1960.
7. Bisplinghoff, Raymond L., Ashley, Holt, and Halfman, Robert L.: Aeroelasticity. Addison-Wesley Pub. Co., Inc. (Cambridge, Mass.), c.1955, pp. 632-694.
8. Diederich, Franklin W., and Zlotnick, Martin: Calculated Spanwise Lift Distributions, Influence Functions, and Influence Coefficients for Unswept Wings in Subsonic Flow. NACA Rep. 1228, 1955. (Supersedes NACA TN 3014.)
9. Jones, W. Prichard: Aerodynamic Forces on Wings in Non-Uniform Motion. R. & M. No. 2117, British A.R.C., Aug. 1945.
10. Diederich, Franklin W., and Zlotnick, Martin: Calculated Spanwise Lift Distributions and Aerodynamic Influence Coefficients for Swept Wings in Subsonic Flow. NACA TN 3476, 1955.

TABLE I.- STEADY-STATE VALUES OF LIFT- AND PITCHING-MOMENT-CURVE SLOPES

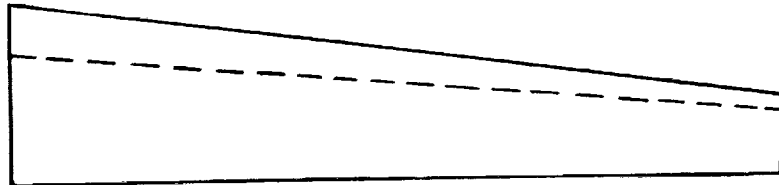
Planform	A	λ_T	M	$dC_L/d\alpha$	$dC_m/d\alpha$
Unswep	6.00	1.00	0	4.28	-----
Unswep	6.00	.50	.40	4.77	2.49
Unswep	6.00	.50	.90	6.90	3.80
5° swept	11.60	.44	.33	6.08	1.17
5° swept	11.60	.44	.70	7.55	1.42
35° swept	4.00	.42	.40	3.74	-1.35
35° swept	4.00	.42	.90	4.78	-1.78
35° swept	9.43	.42	.58	5.06	-7.94
35° swept	9.43	.42	.90	6.32	-10.17
60° delta	2.30	0	.40	2.63	-.42
60° delta	2.30	0	.90	3.07	-.63
75° delta	1.07	0	.40	1.46	-.30
75° delta	1.07	0	.90	1.57	-.40



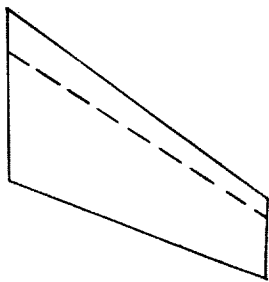
Un swept
 $A = 6.00$
 $\lambda_T = 1.00$



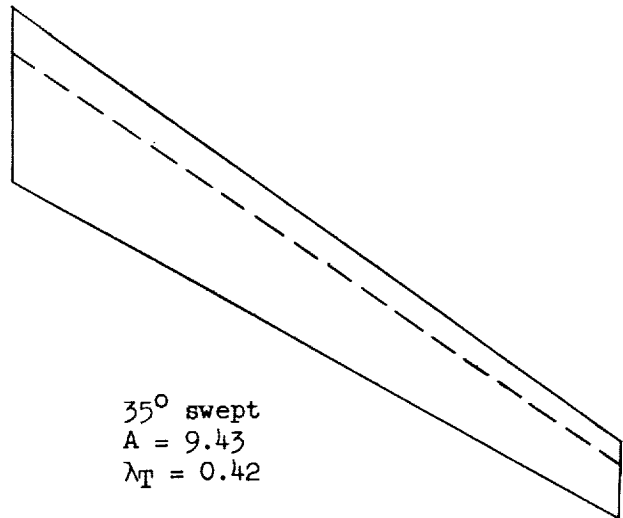
Un swept
 $A = 6.00$
 $\lambda_T = 0.50$



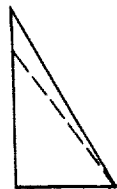
5° swept
 $A = 11.60$
 $\lambda_T = 0.44$



35° swept
 $A = 4.00$
 $\lambda_T = 0.42$



35° swept
 $A = 9.43$
 $\lambda_T = 0.42$

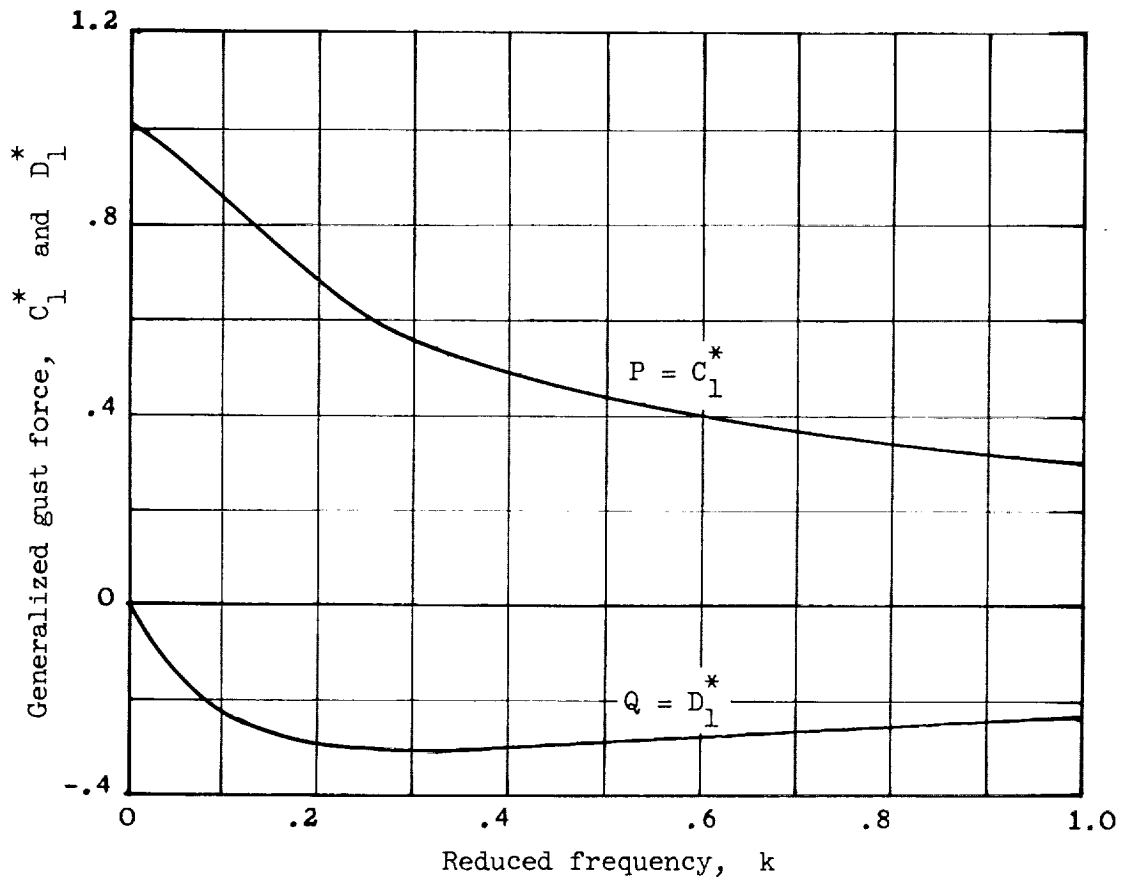


60° delta
 $A = 2.30$
 $\lambda_T = 0$



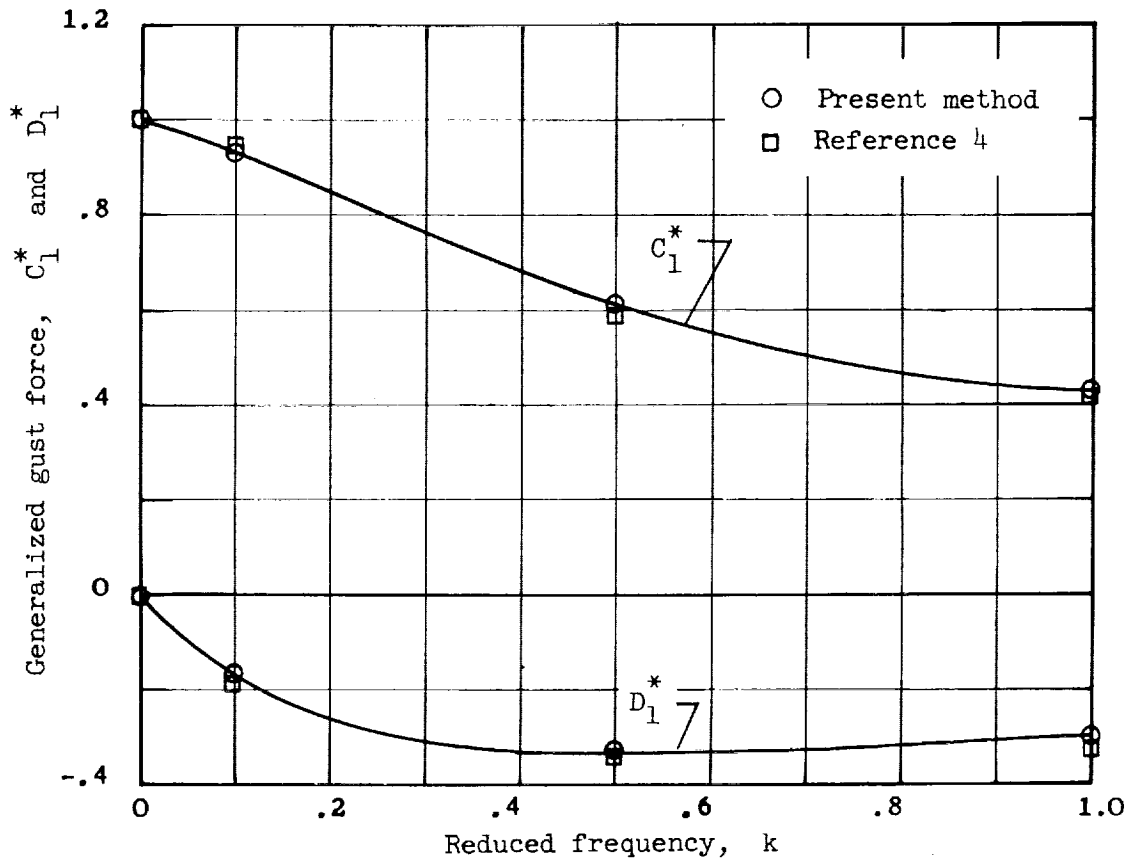
75° delta
 $A = 1.07$
 $\lambda_T = 0$

Figure 1.- Sketches of semispans of wing planforms considered (shown for uniform root chord).



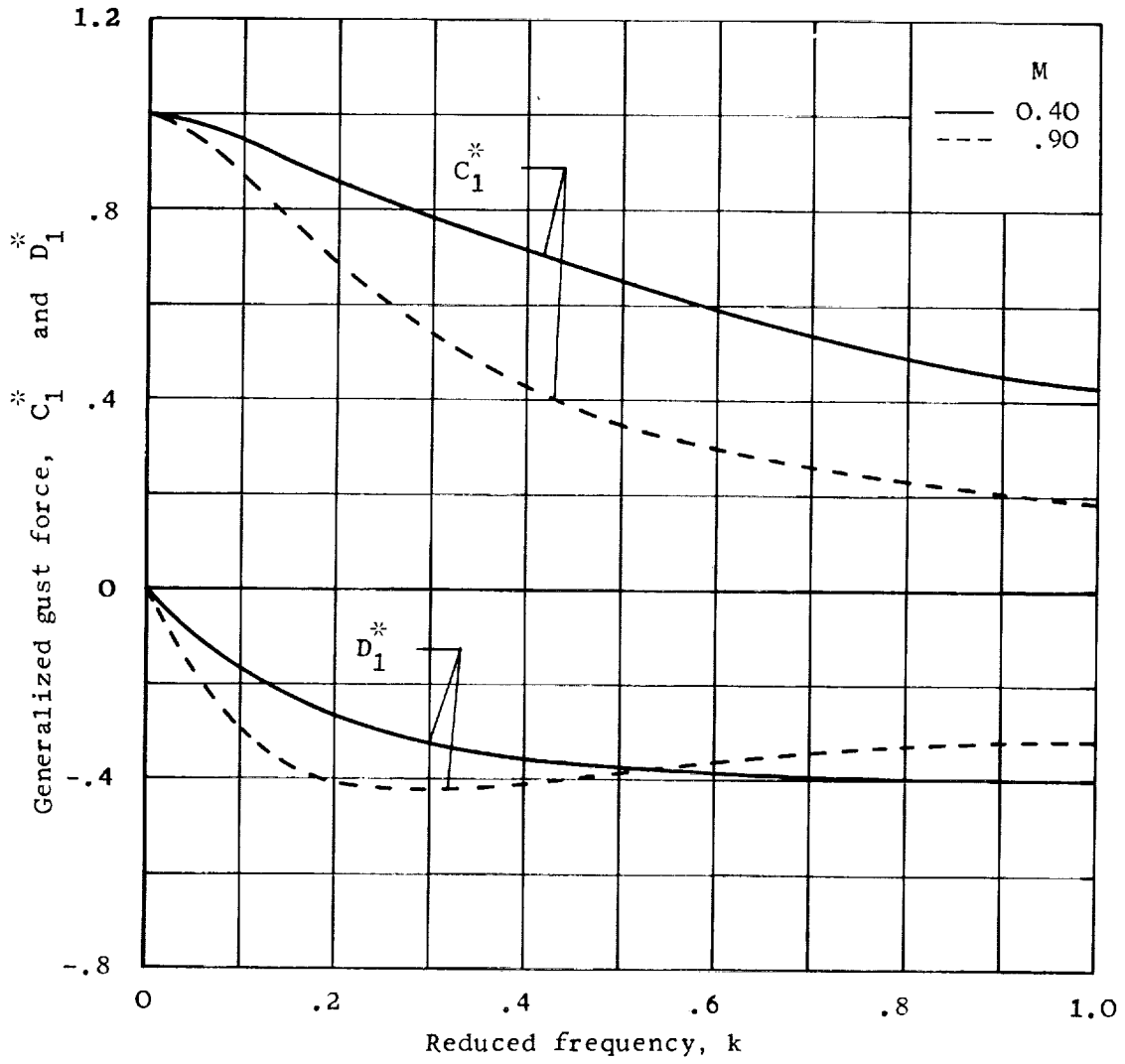
(a) The two-dimensional wing ($A = \infty$) in incompressible flow ($M = 0$).
 (C_1^* and D_1^* are the P and Q functions, data given in ref. 1.)

Figure 2.- The variation with reduced frequency k of the in-phase (real) and quadrature (imaginary) components of the generalized gust force tending to produce vertical translation (equivalent to total lift), normalized by the force magnitude for $k = 0$, for the various wing planforms shown in figure 1 at Mach number M in a continuous sinusoidal gust field. The phase referral is to the gust velocity at the wing apex.



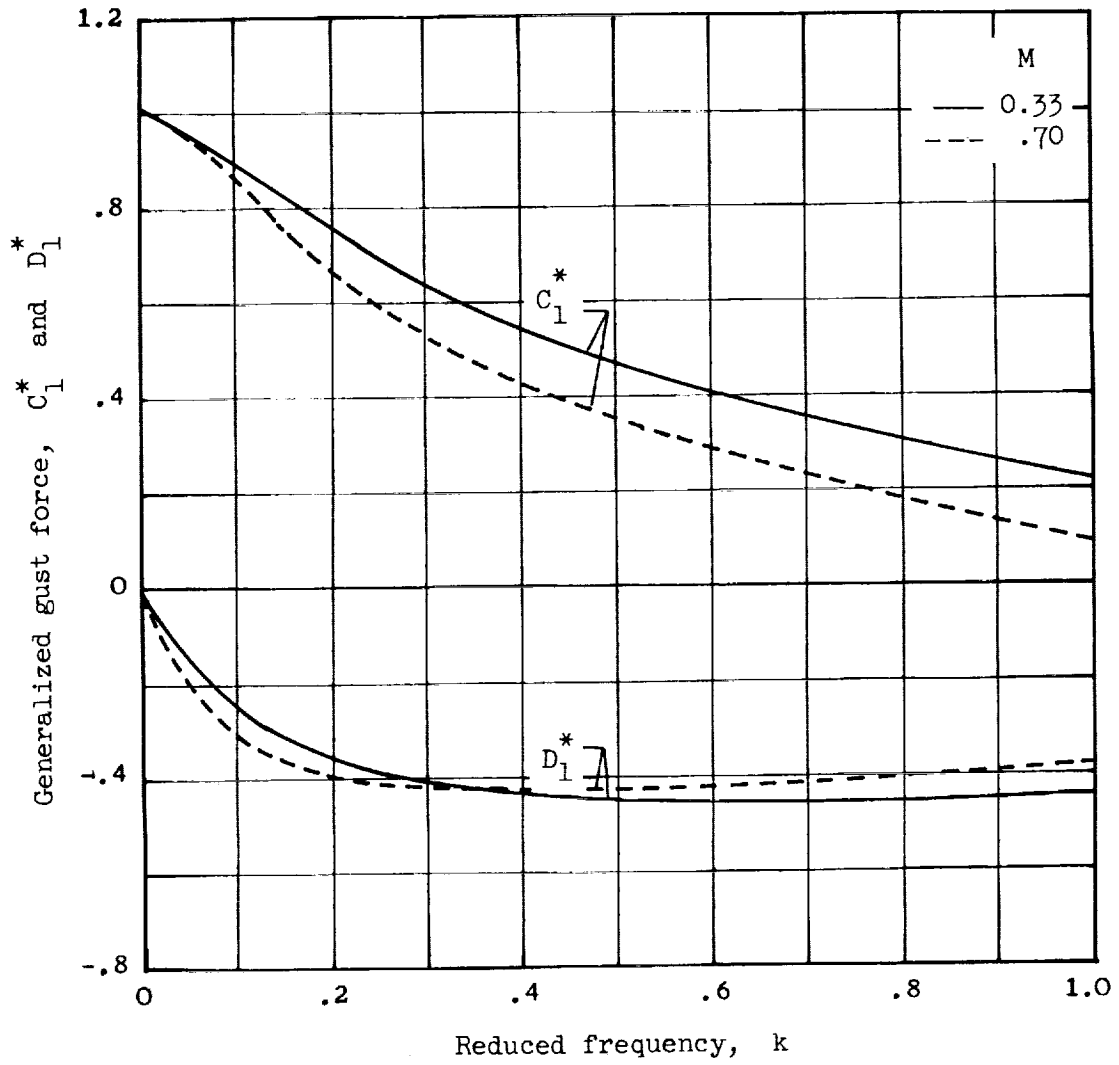
(b) Unswept wing; $A = 6.00$; $\lambda_T = 1.00$; $M = 0$.

Figure 2.- Continued.



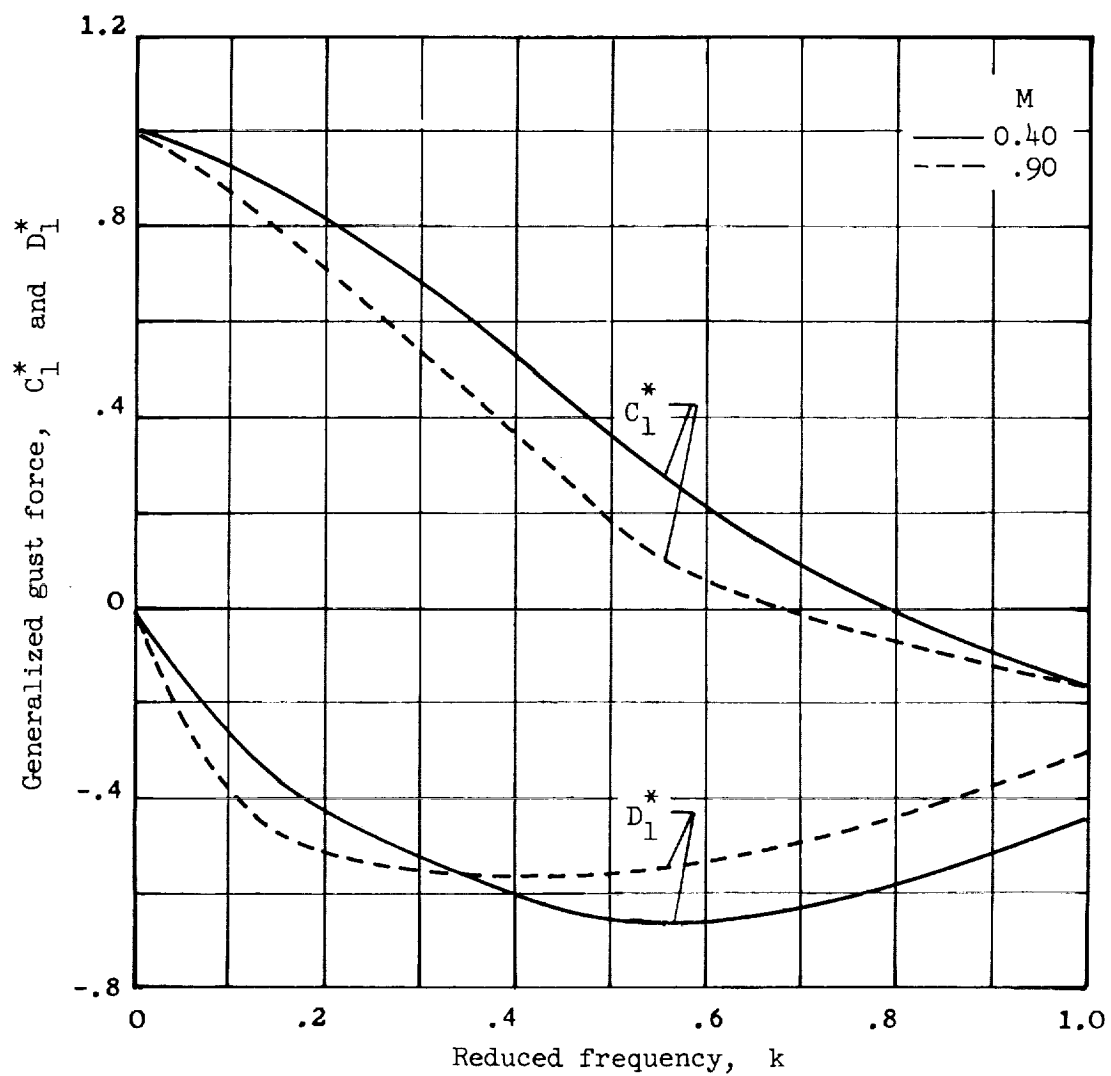
(c) Unswept wing; $A = 6.00$; $\lambda_T = 0.50$.

Figure 2.- Continued.



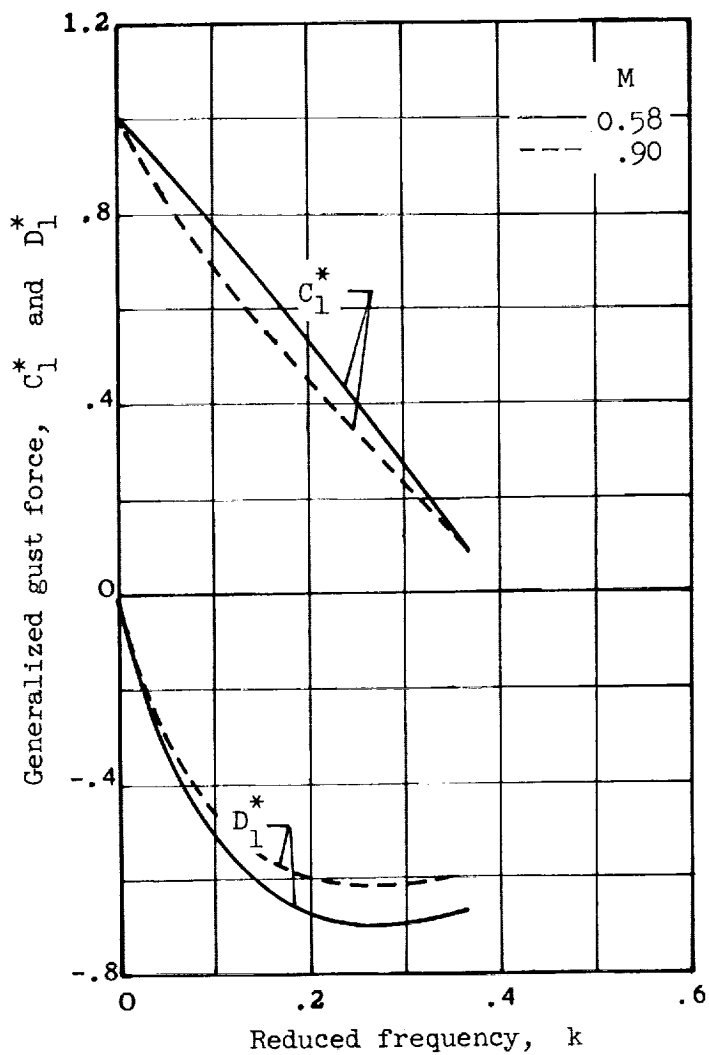
(d) 5° swept wing; $A = 11.60$; $\lambda_T = 0.44$.

Figure 2.- Continued.



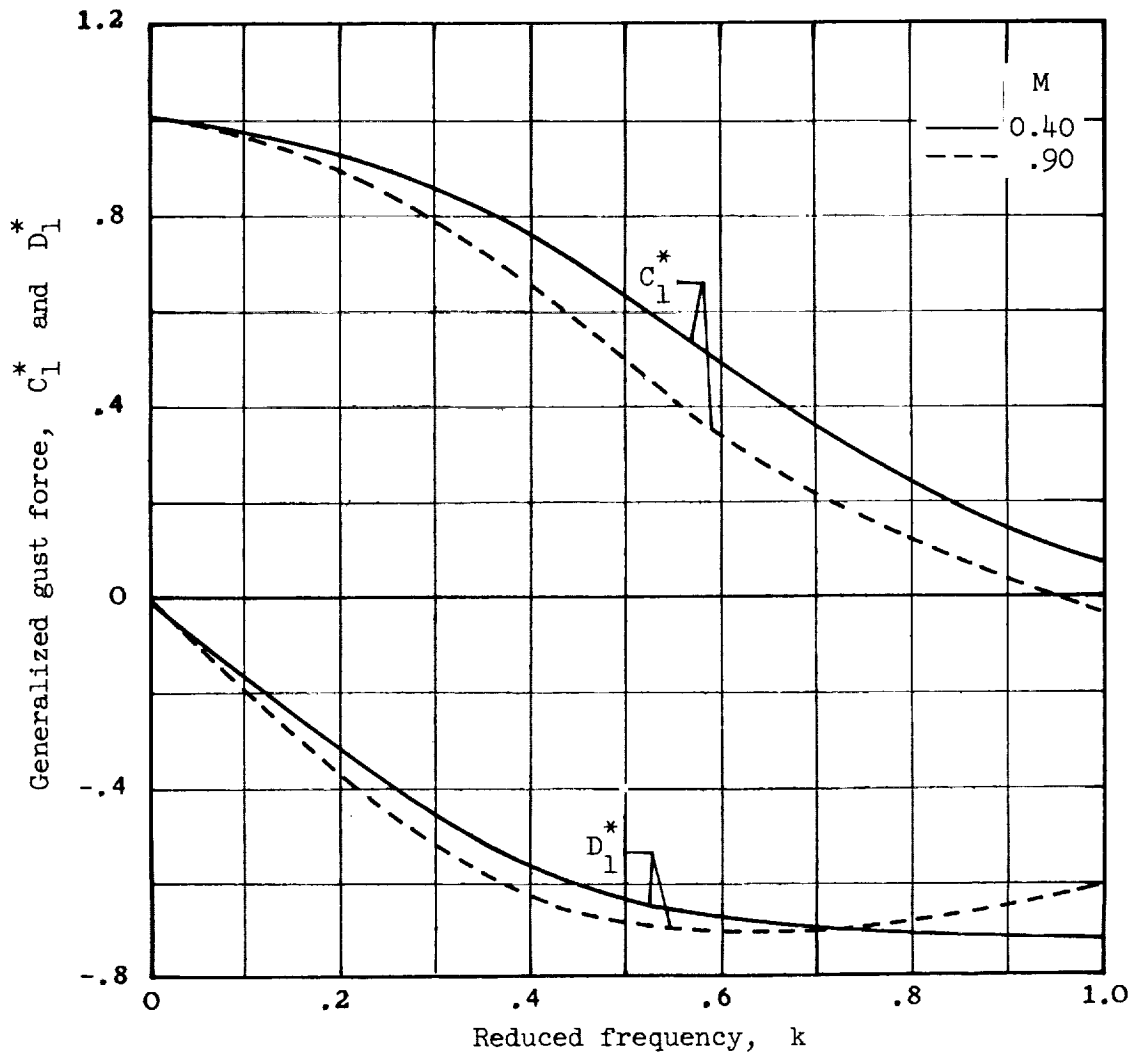
(e) 35° swept wing; $A = 4.00$; $\lambda_T = 0.42$.

Figure 2.- Continued.



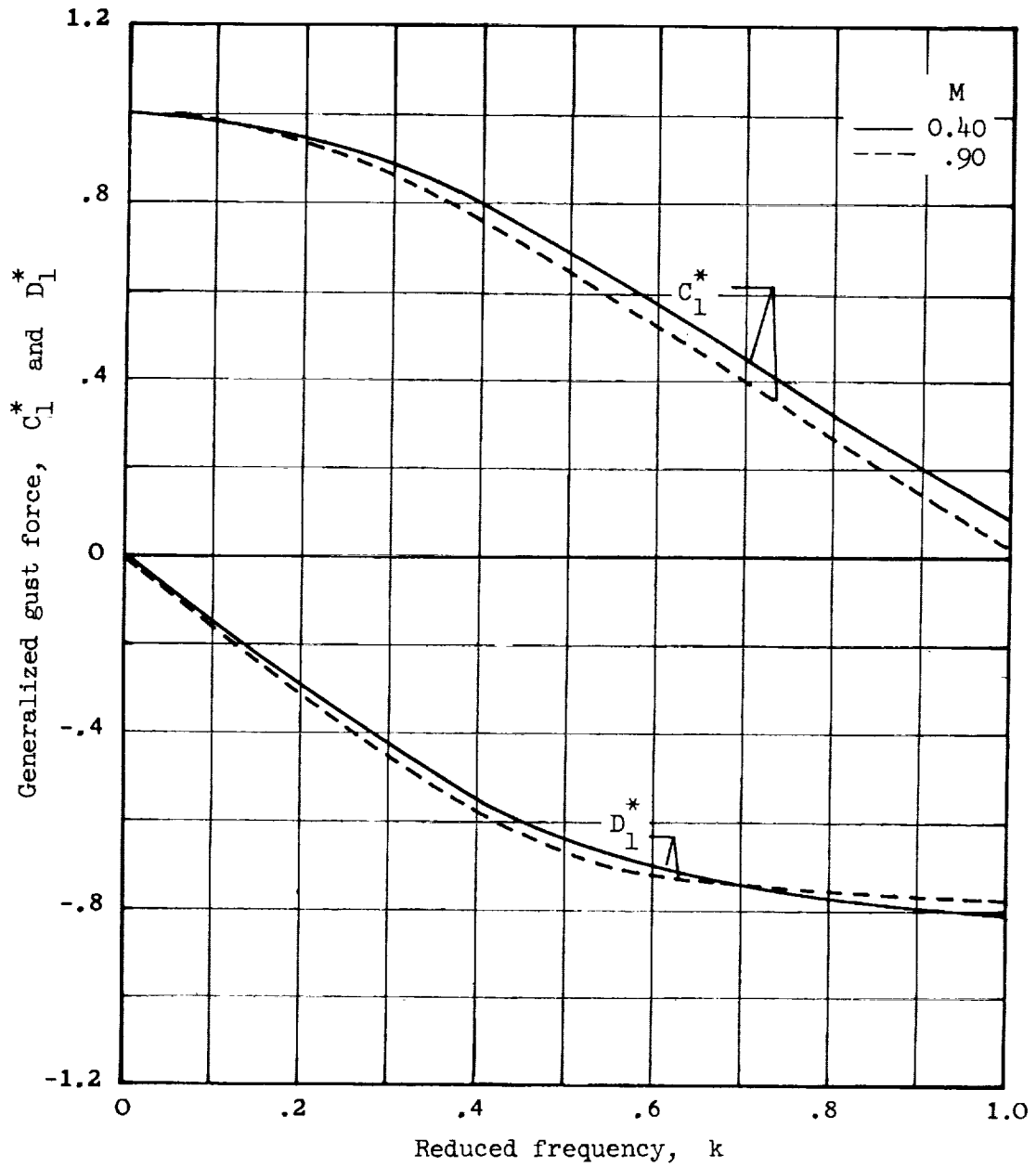
(f) 35° swept wing; $A = 9.43$; $\lambda_T = 0.42$.

Figure 2.- Continued.



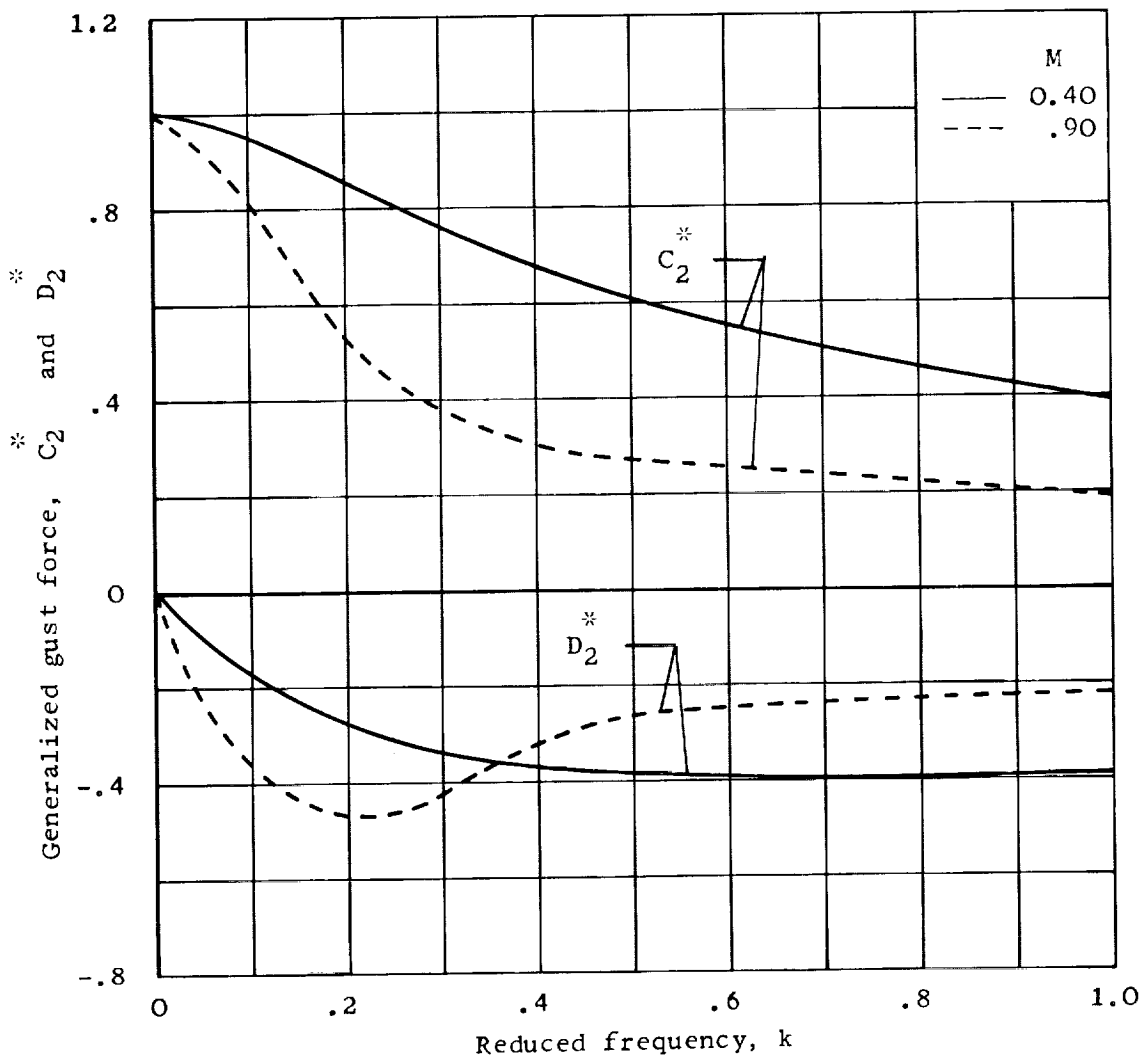
(g) 60° delta wing; $A = 2.30$; $\lambda_T = 0$.

Figure 2.- Continued.



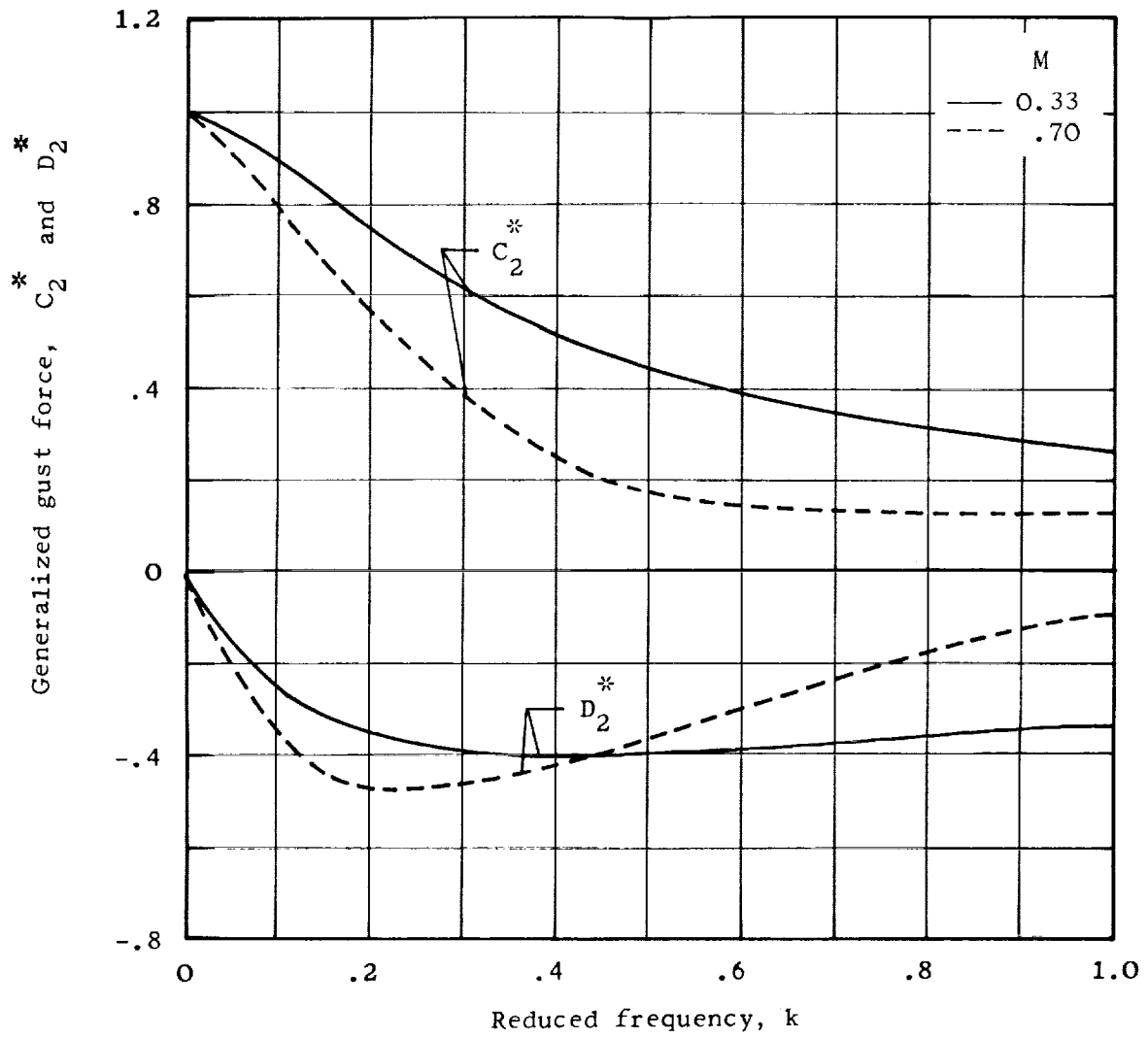
(h) 75° delta wing; $A = 1.07$; $\lambda_T = 0$.

Figure 2.- Concluded.



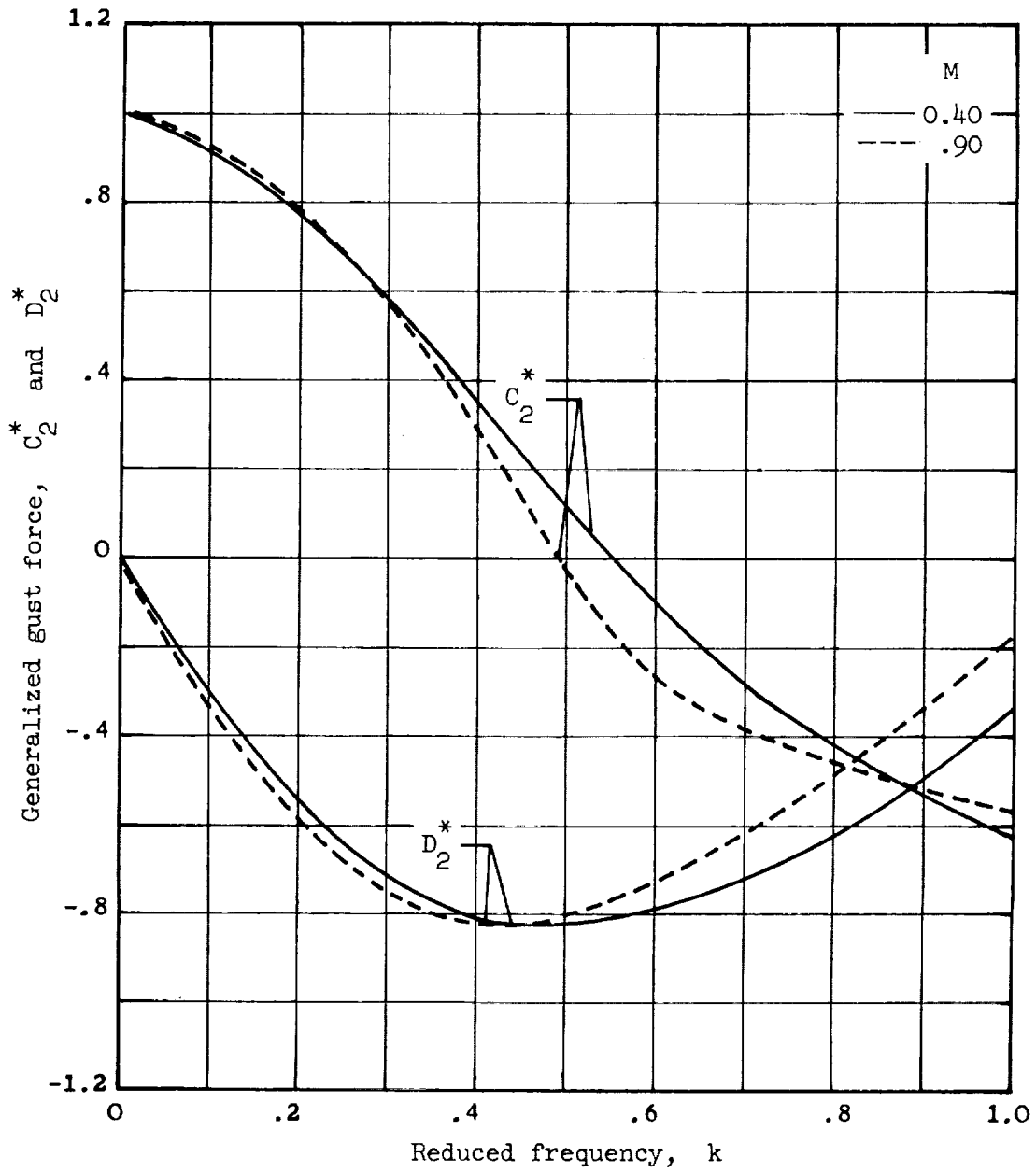
(a) Unswept wing; $A = 6.00$; $\lambda_T = 0.50$.

Figure 3.- The variation with reduced frequency k of the in-phase and quadrature components of the generalized gust force tending to produce a displacement in pitch about an axis through the root midchord (equivalent to total pitching moment), normalized by the force magnitude for $k = 0$, for the wings of figure 1 in a continuous sinusoidal gust field. The phase referral is to the gust velocity at the wing apex.



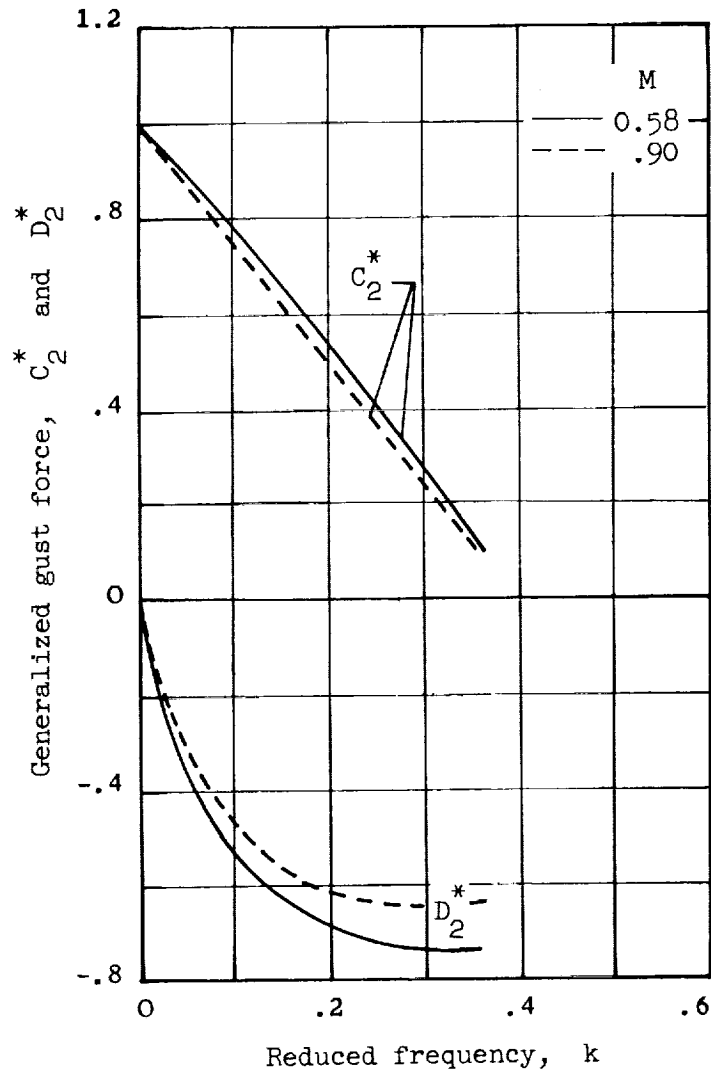
(b) 5° swept wing; $A = 11.60$; $\lambda_T = 0.44$.

Figure 3.- Continued.



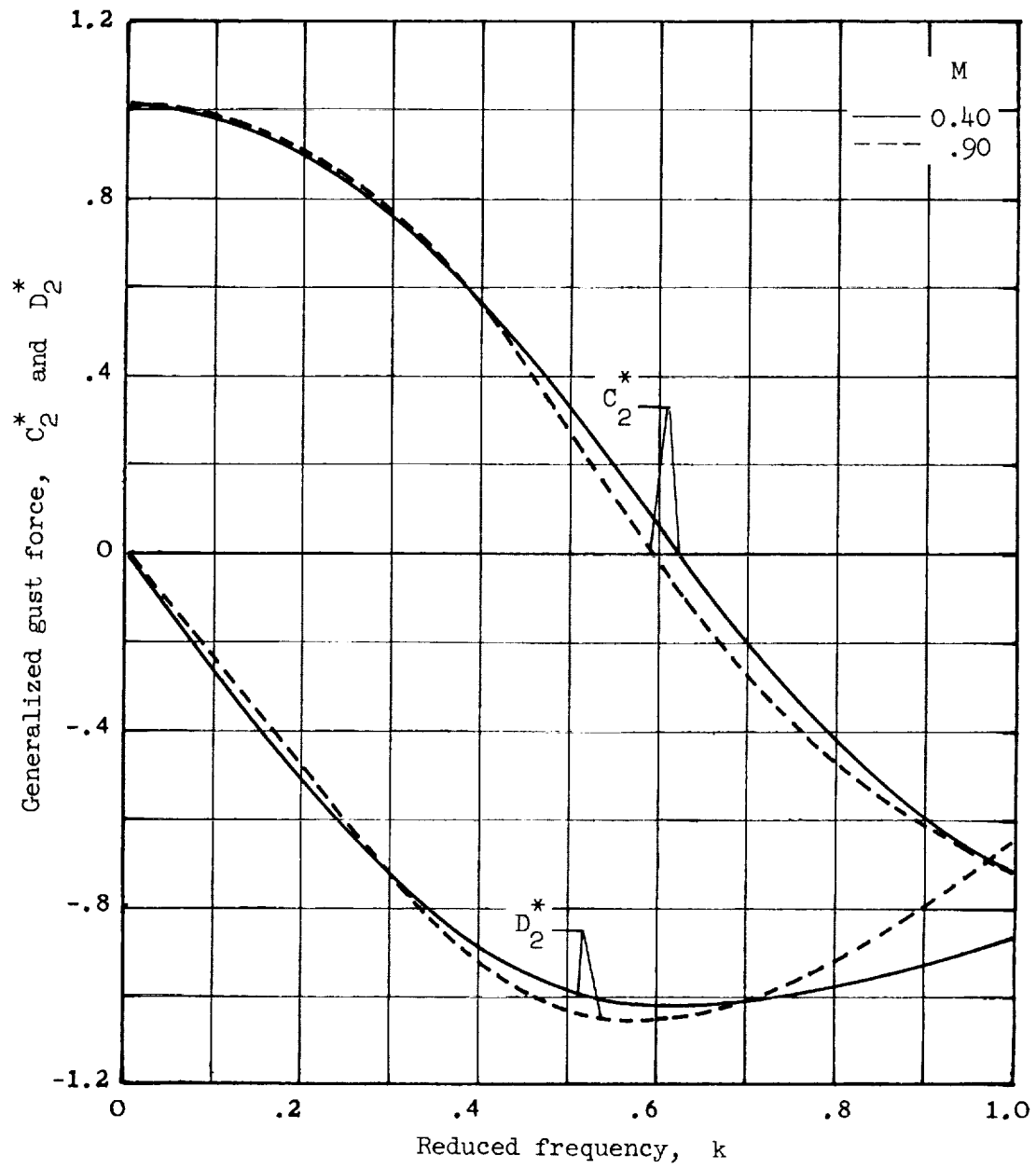
(c) 35° swept wing; $A = 4.00$; $\lambda_T = 0.42$.

Figure 3.- Continued.



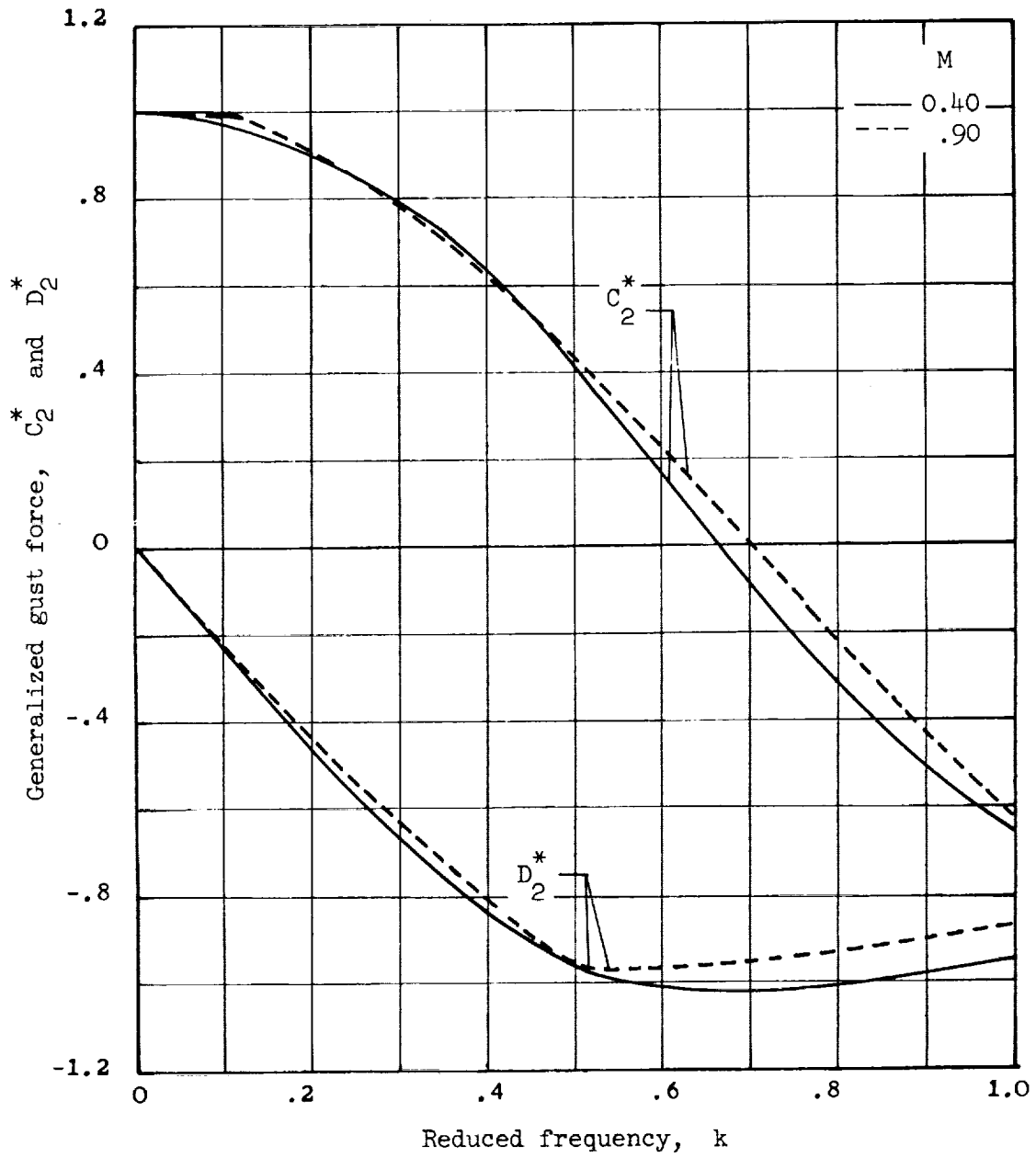
(d) 35° swept wing; $A = 9.43$; $\lambda_T = 0.42$.

Figure 3.- Continued.



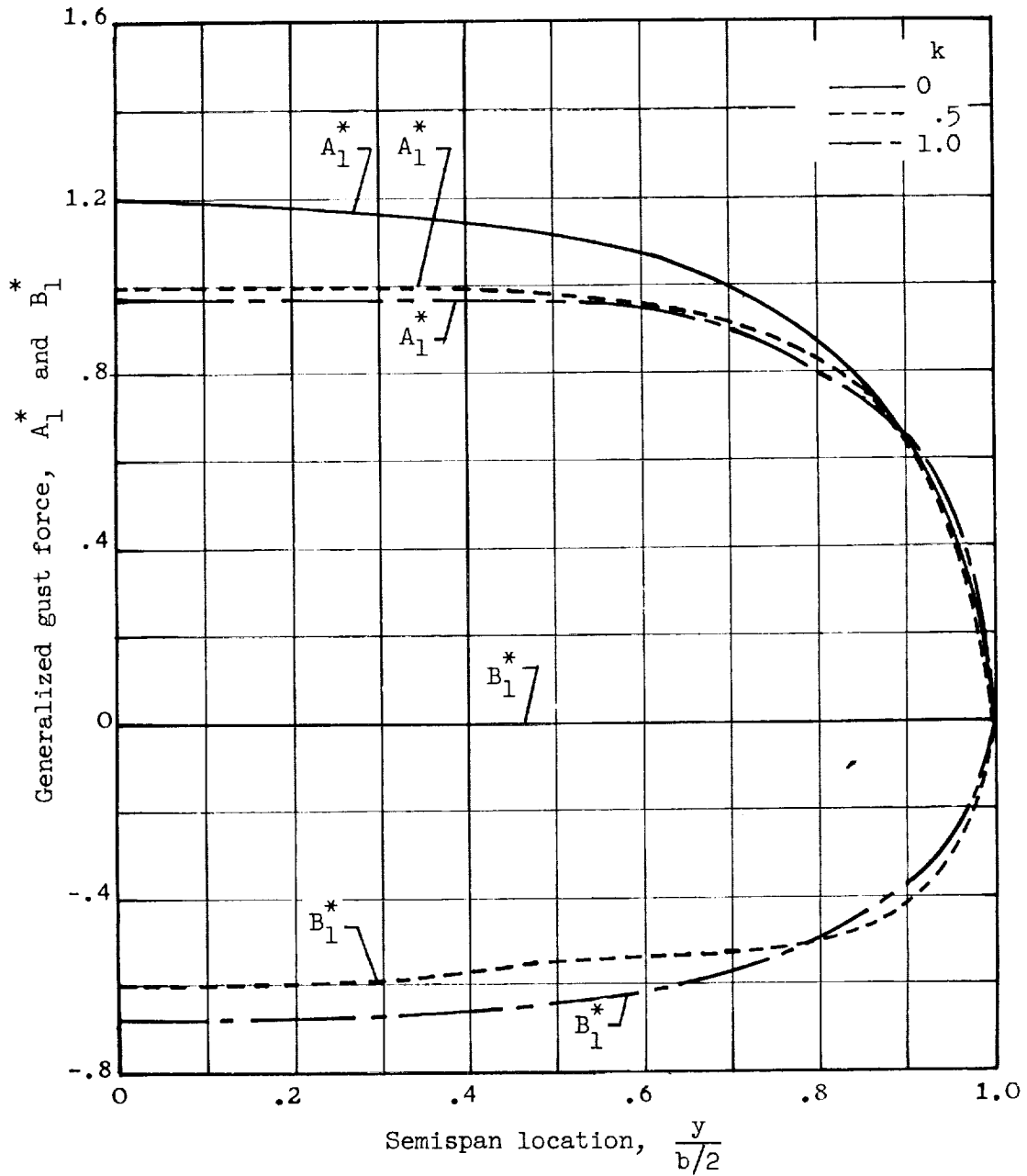
(e) 60° delta wing; $A = 2.30$; $\lambda_T = 0$.

Figure 3.- Continued.



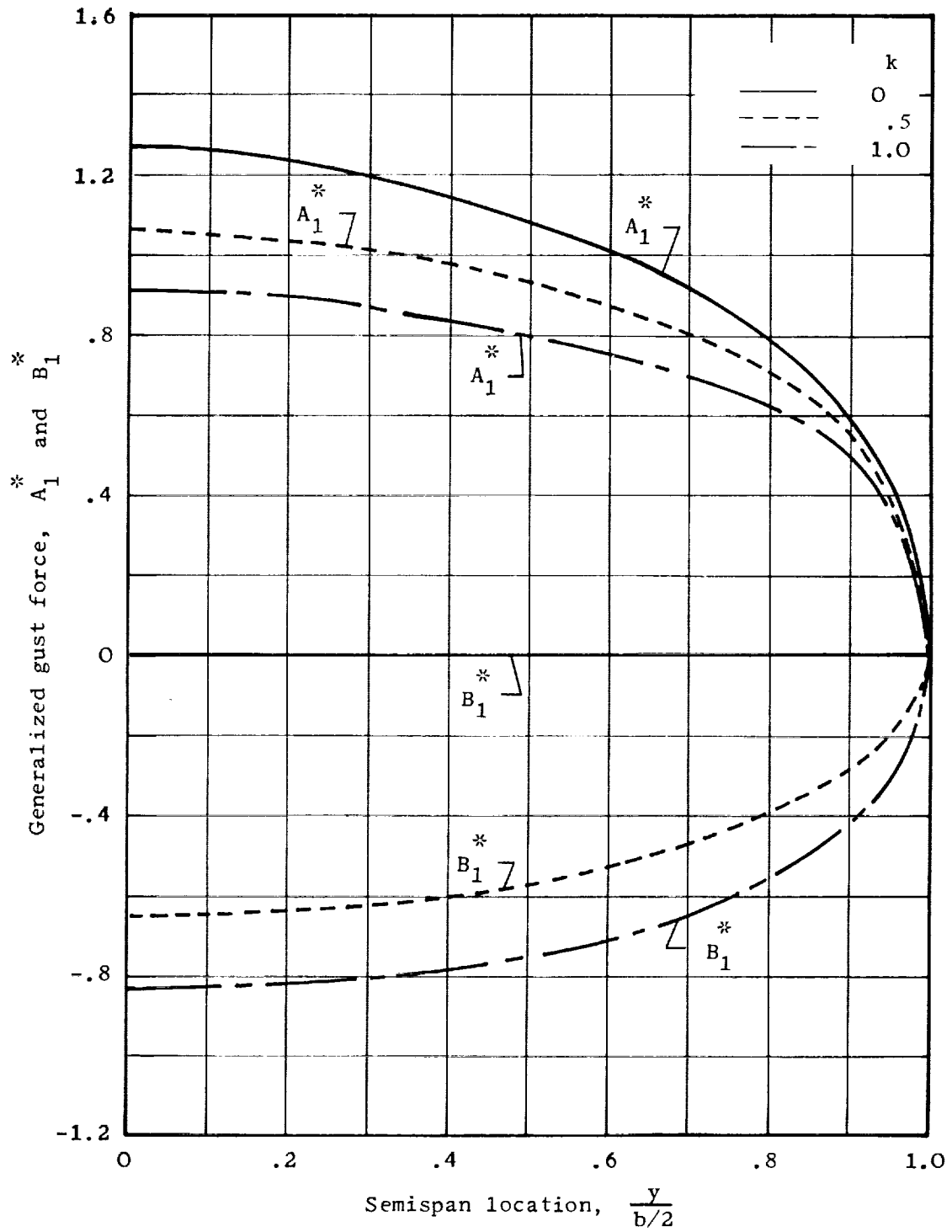
(f) 75° delta wing; $A = 1.07$; $\lambda_T = 0$.

Figure 3.- Concluded.



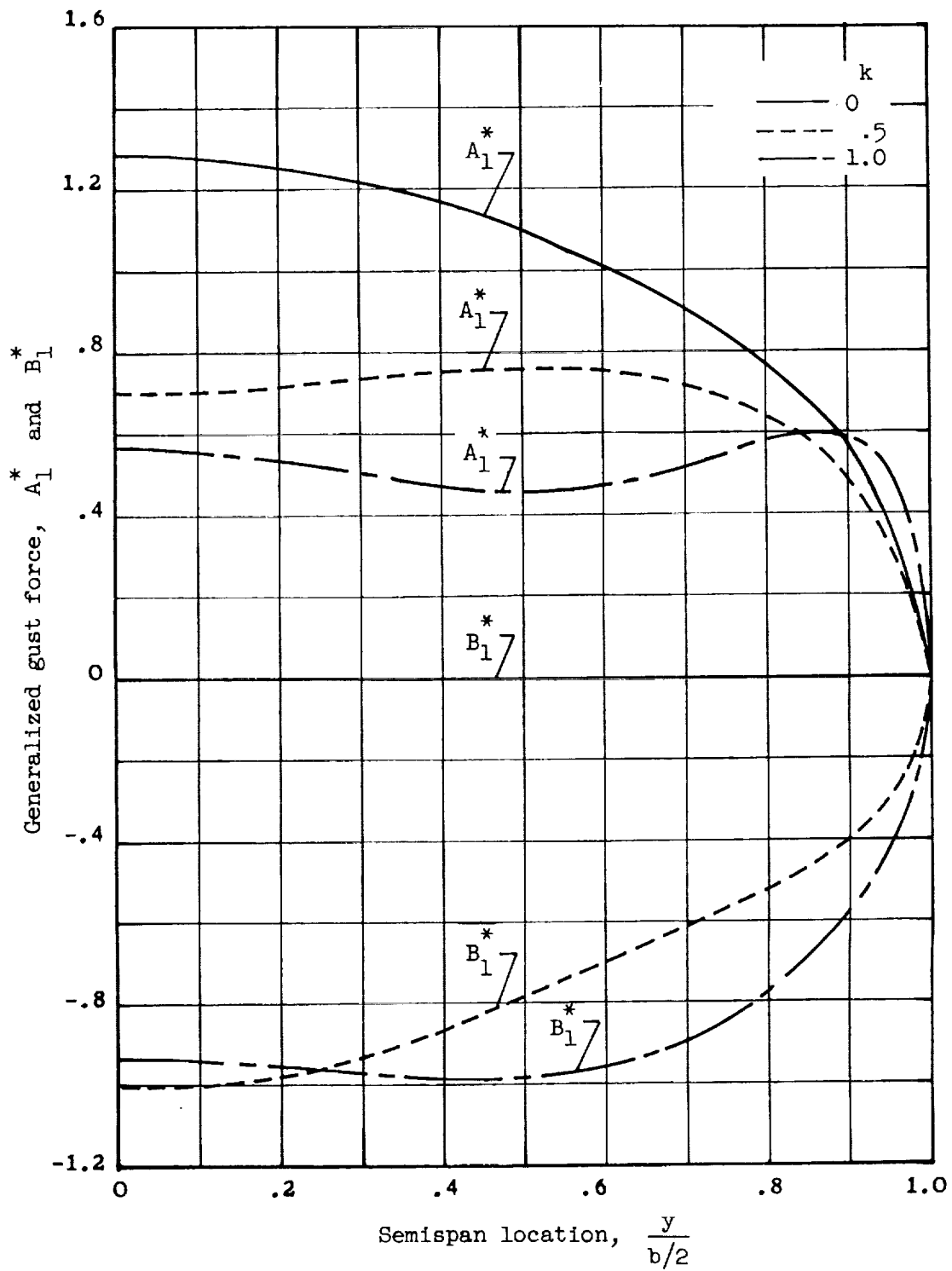
(a) Unswept wing; $A = 6.00$; $\lambda_T = 1.00$; $M = 0$.

Figure 4.- Spanwise distribution of the in-phase and quadrature components of the generalized gust force tending to produce vertical translation (equivalent to section lift), normalized by division by the magnitude of the total lift $\sqrt{C_1^2 + D_1^2}$, at each value of k for a continuous sinusoidal gust field.



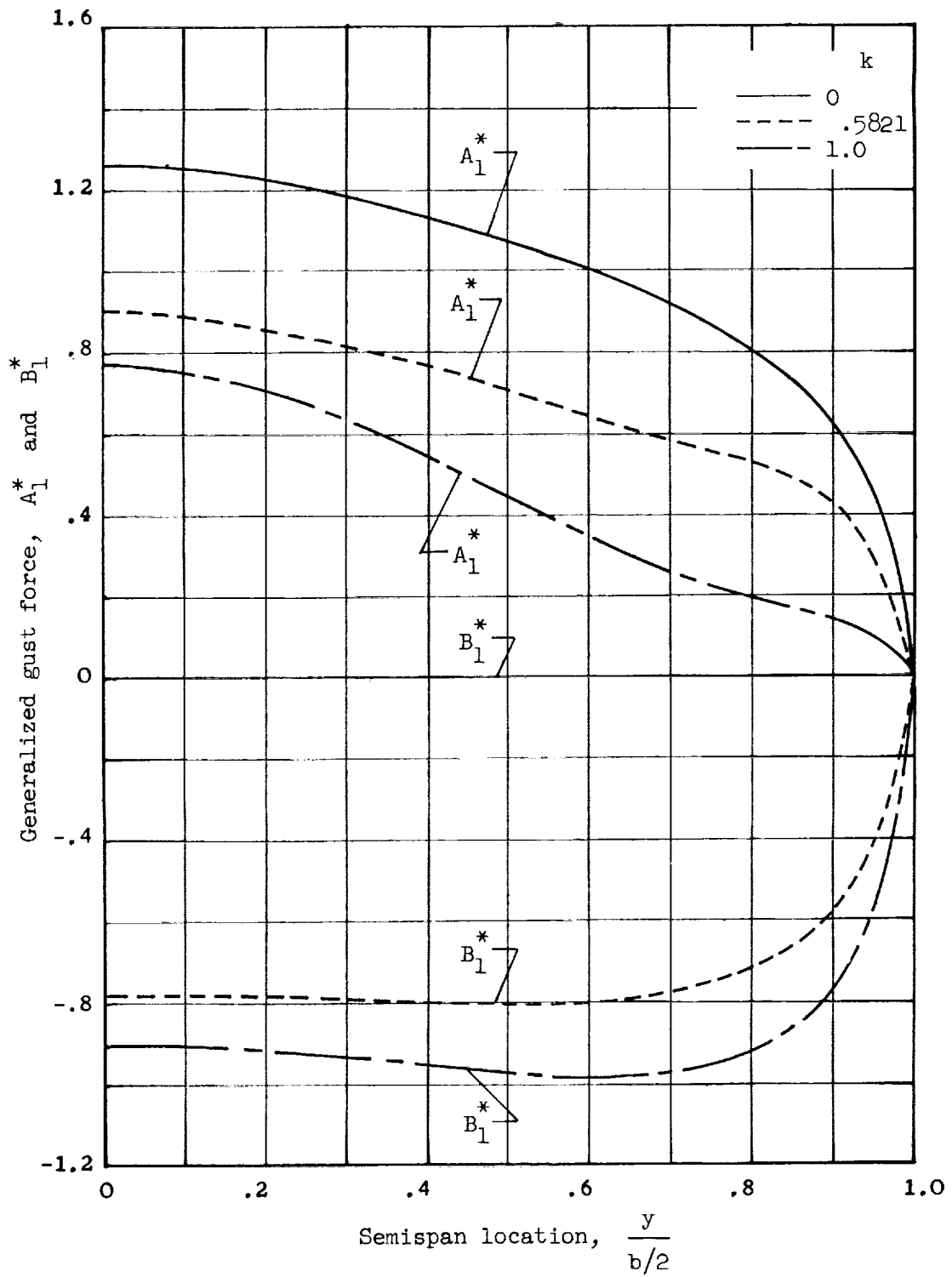
(b) Unswept wing; $A = 6.00$; $\lambda_T = 0.50$; $M = 0.4$.

Figure 4.- Continued.



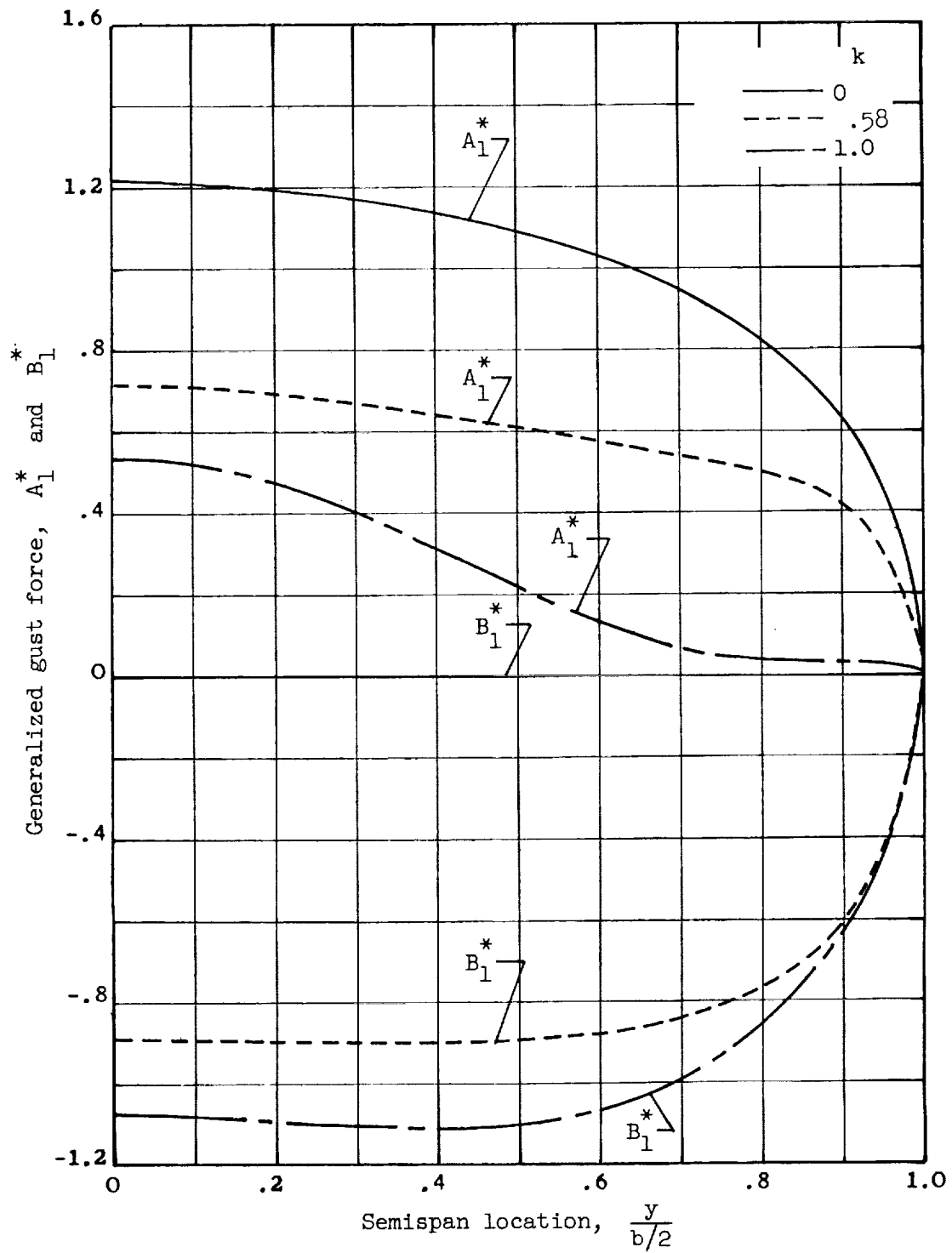
(c) Unswept wing; $A = 6.00$; $\lambda_T = 0.50$; $M = 0.9$.

Figure 4.- Continued.



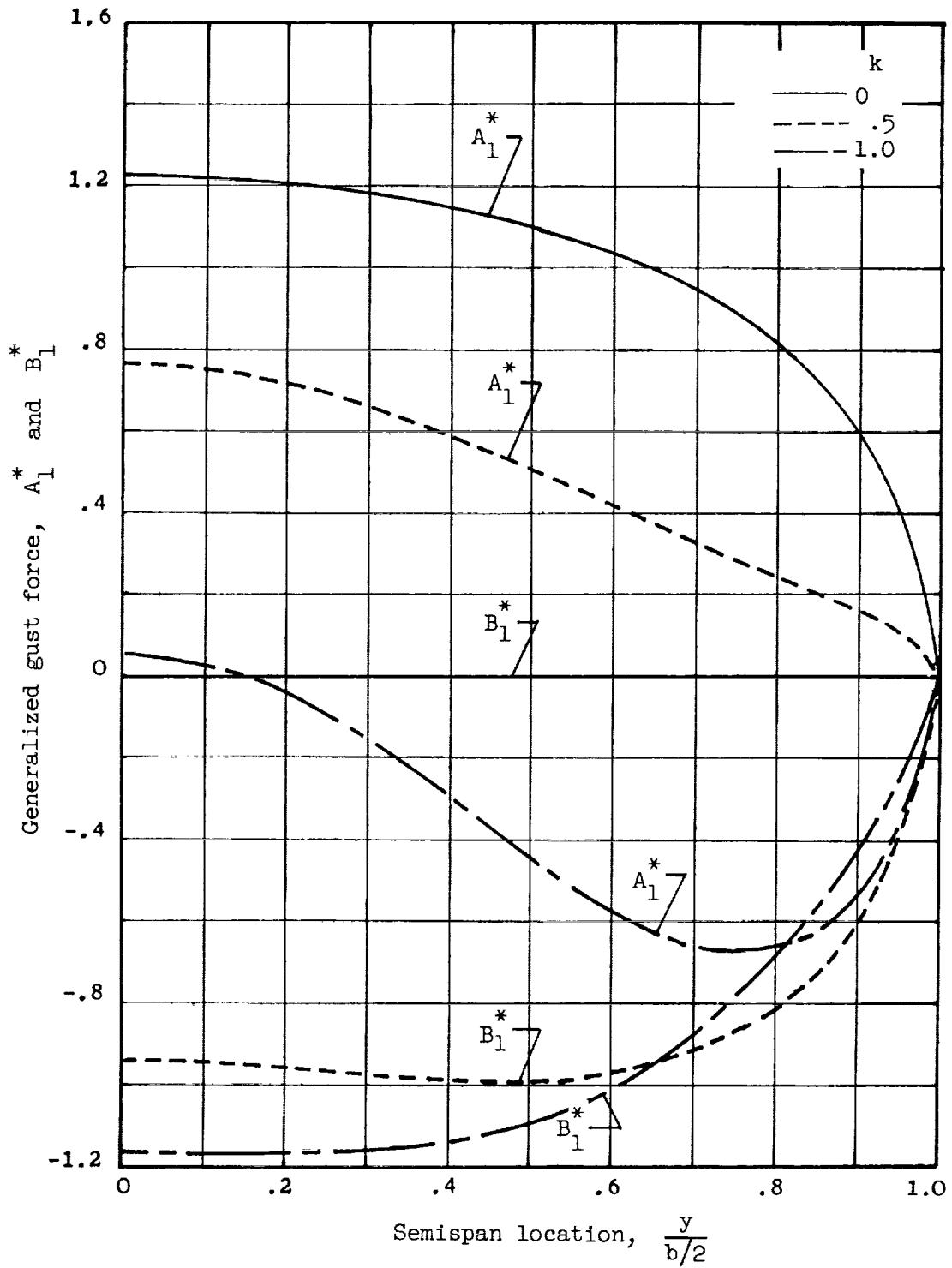
(d) 5° swept wing; $A = 11.60$; $\lambda_T = 0.44$; $M = 0.33$.

Figure 4.- Continued.



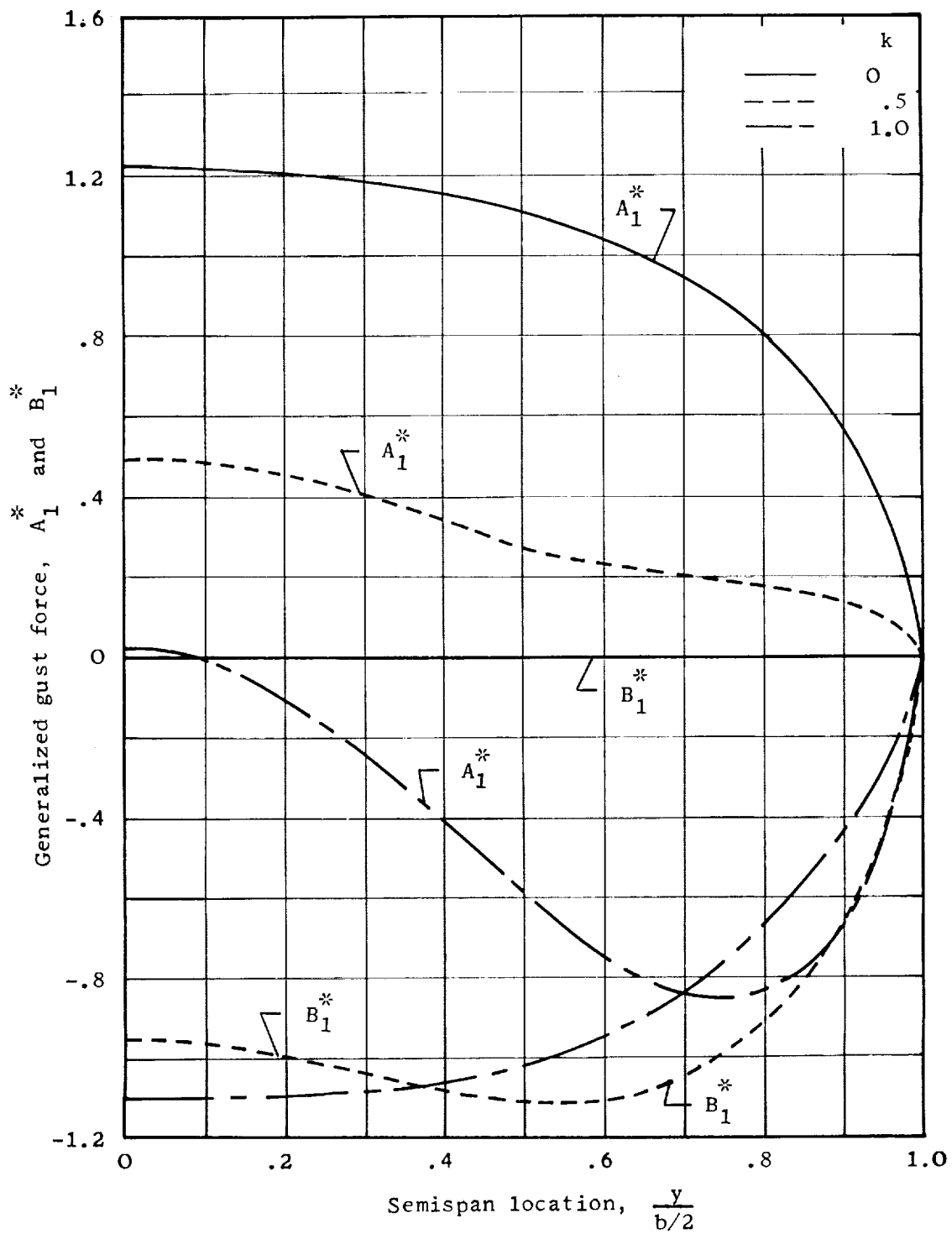
(e) 5° swept wing; $A = 11.60$; $\lambda_T = 0.44$; $M = 0.70$.

Figure 4.- Continued.



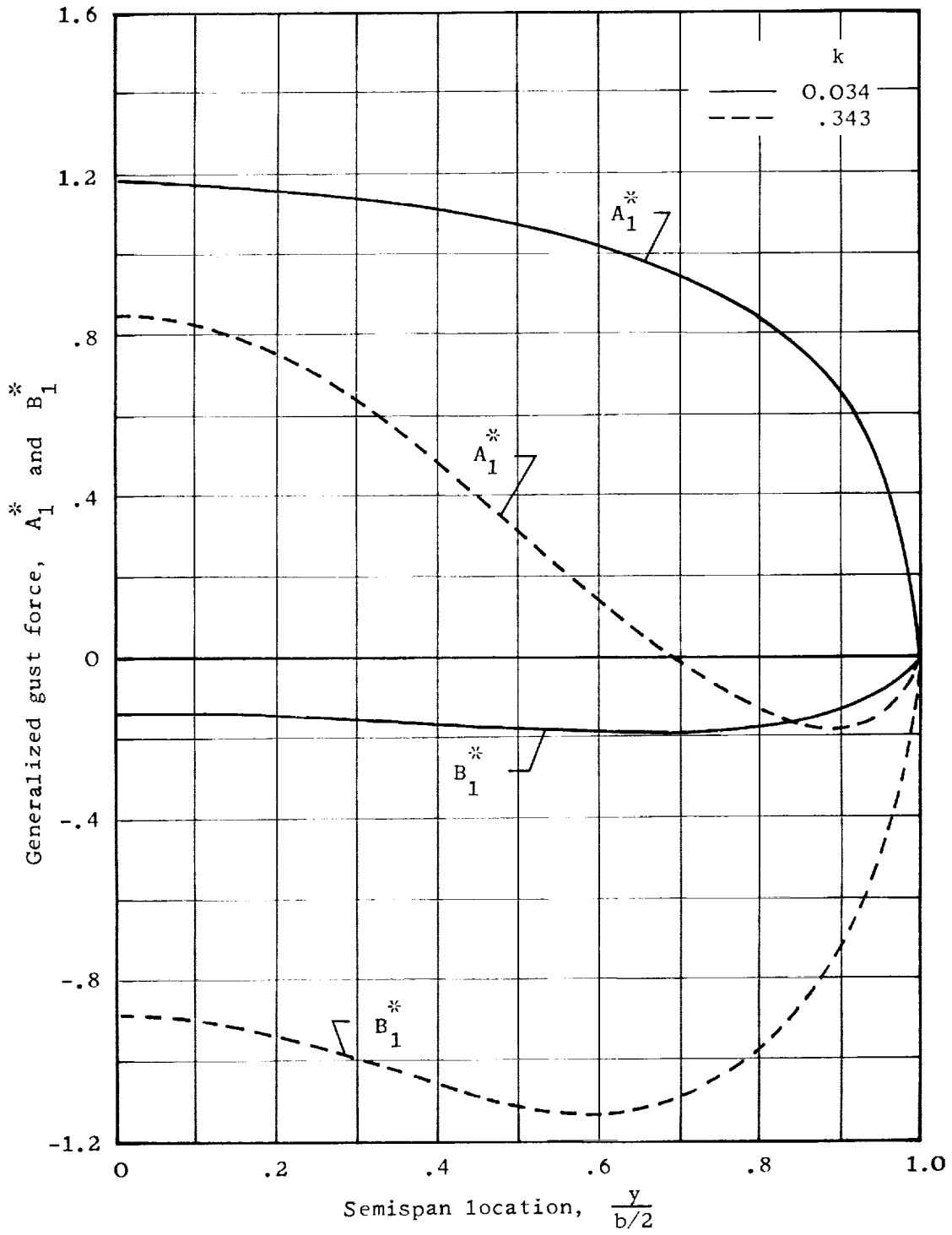
(f) 35° swept wing; $A = 4.00$; $\lambda_T = 0.42$; $M = 0.40$.

Figure 4.- Continued.



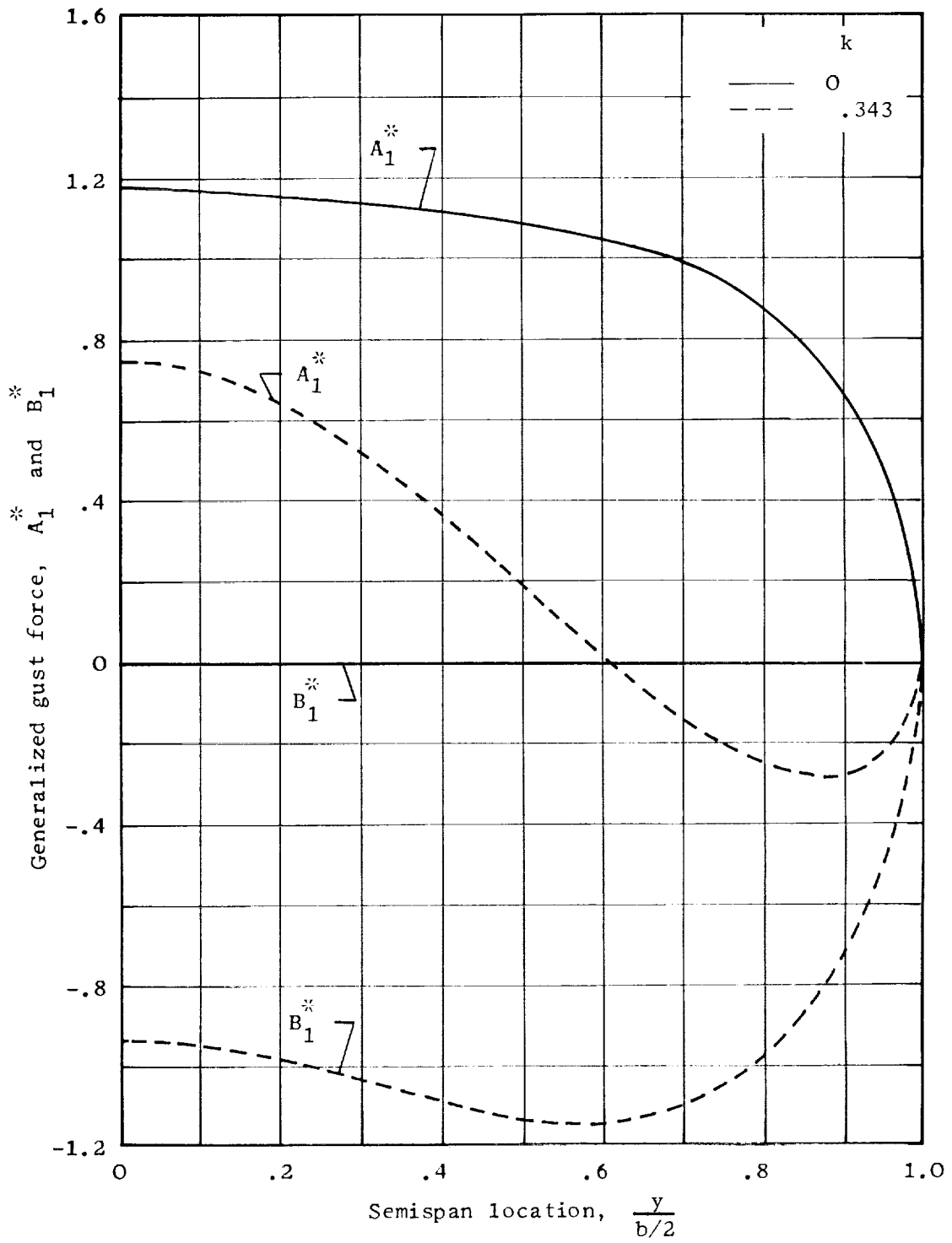
(g) 35° swept wing; $A = 4.00$; $\lambda_{\Gamma} = 0.42$; $M = 0.90$.

Figure 4.- Continued.



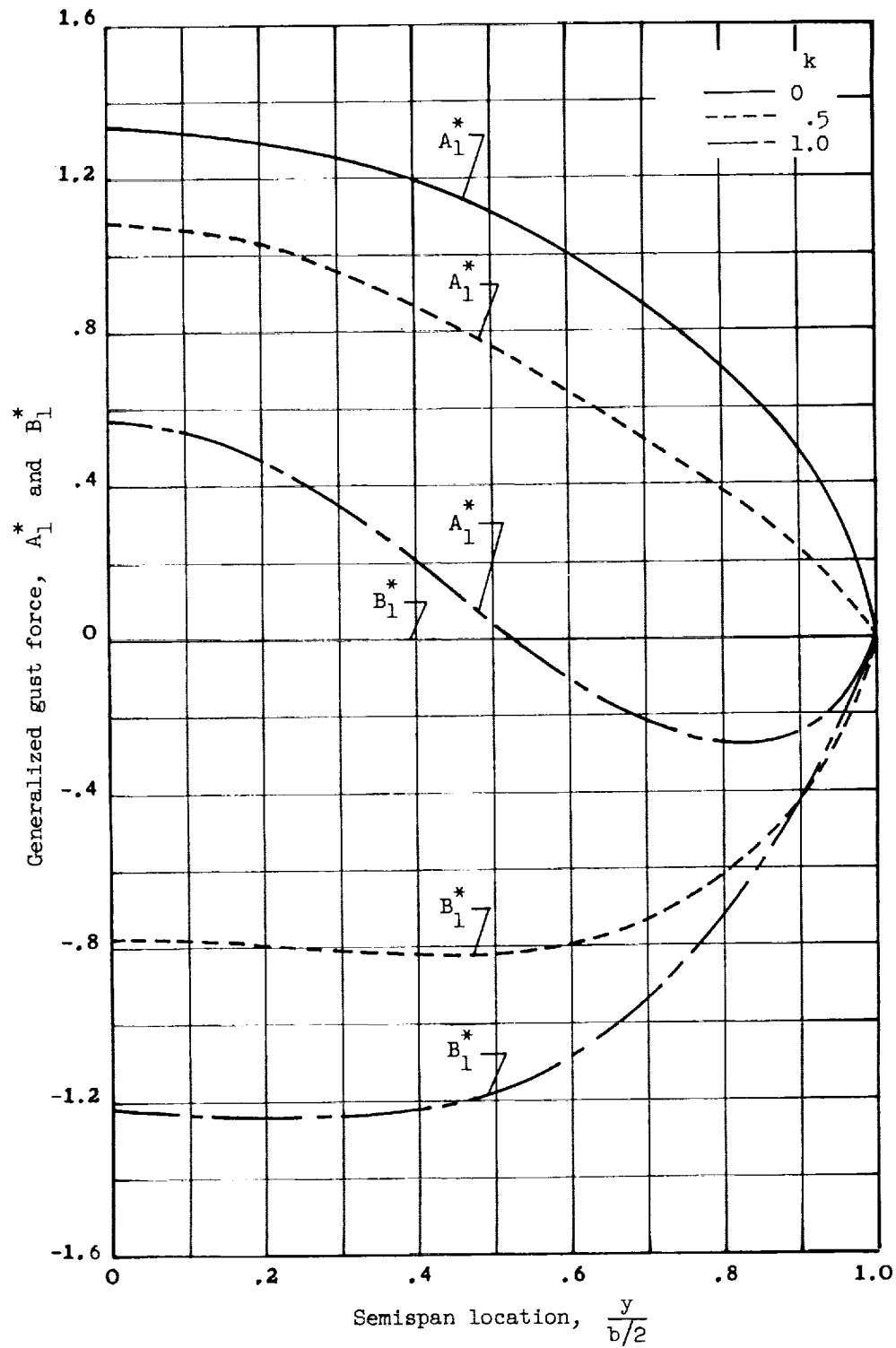
(h) 35° swept wing; $A = 9.43$; $\lambda_T = 0.42$; $M = 0.58$.

Figure 4.- Continued.



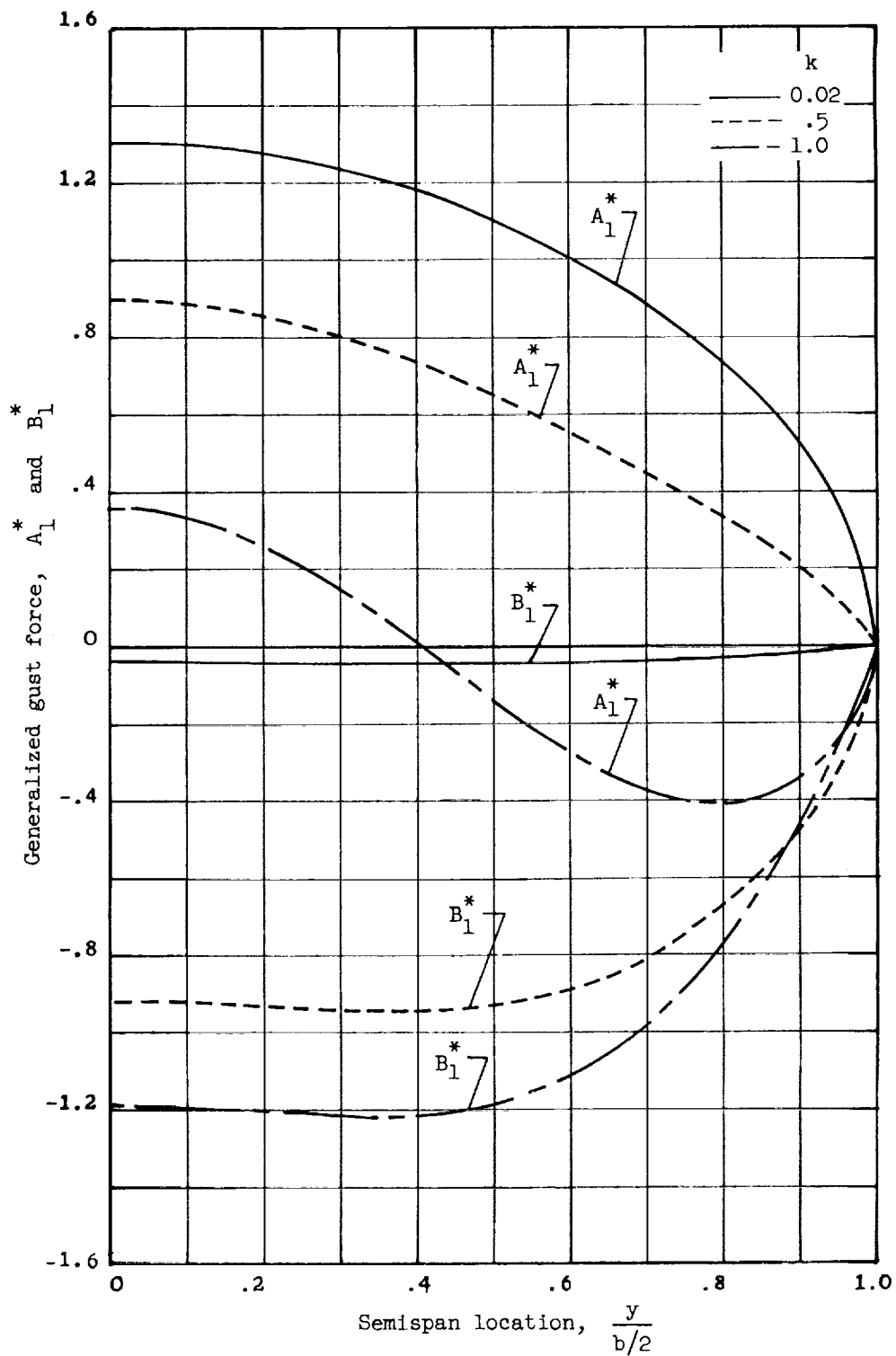
(i) 35° swept wing; $A = 9.43$; $\lambda_T = 0.42$; $M = 0.90$.

Figure 4.- Continued.



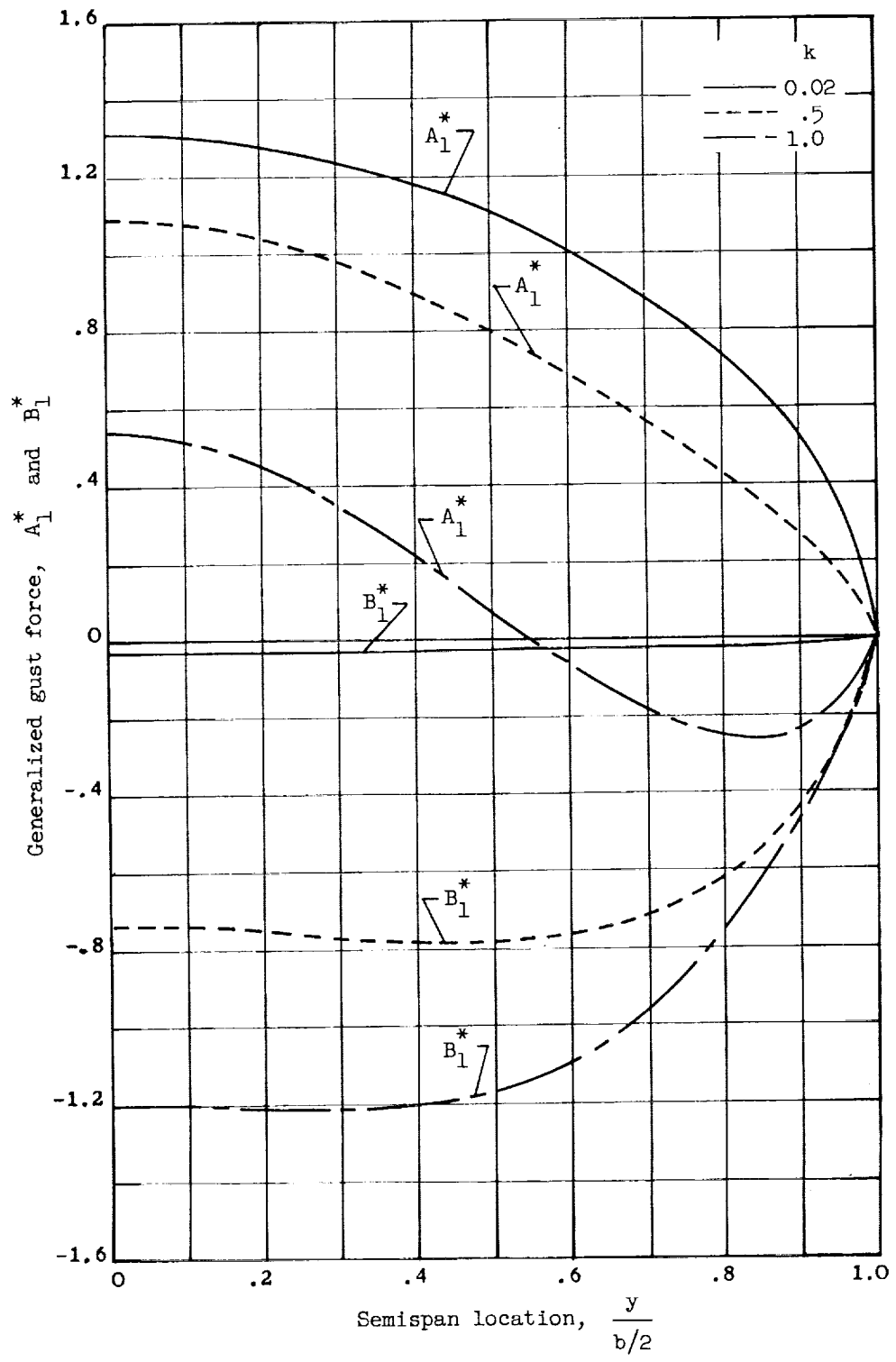
(j) 60° delta wing; $A = 2.30$; $\lambda_T = 0$; $M = 0.40$.

Figure 4.- Continued.



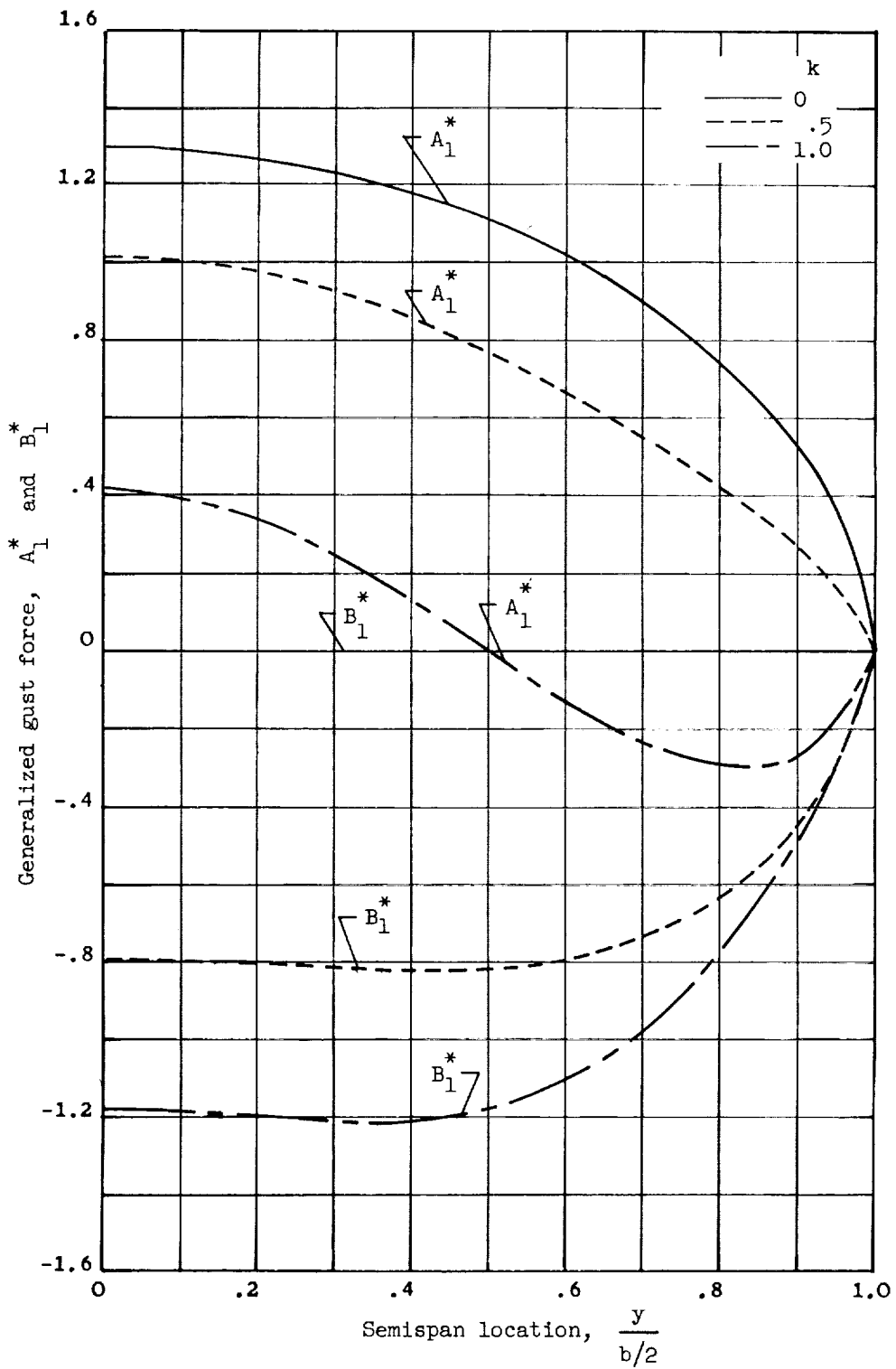
(k) 60° delta wing; $A = 2.30$; $\lambda_T = 0$; $M = 0.90$.

Figure 4.- Continued.



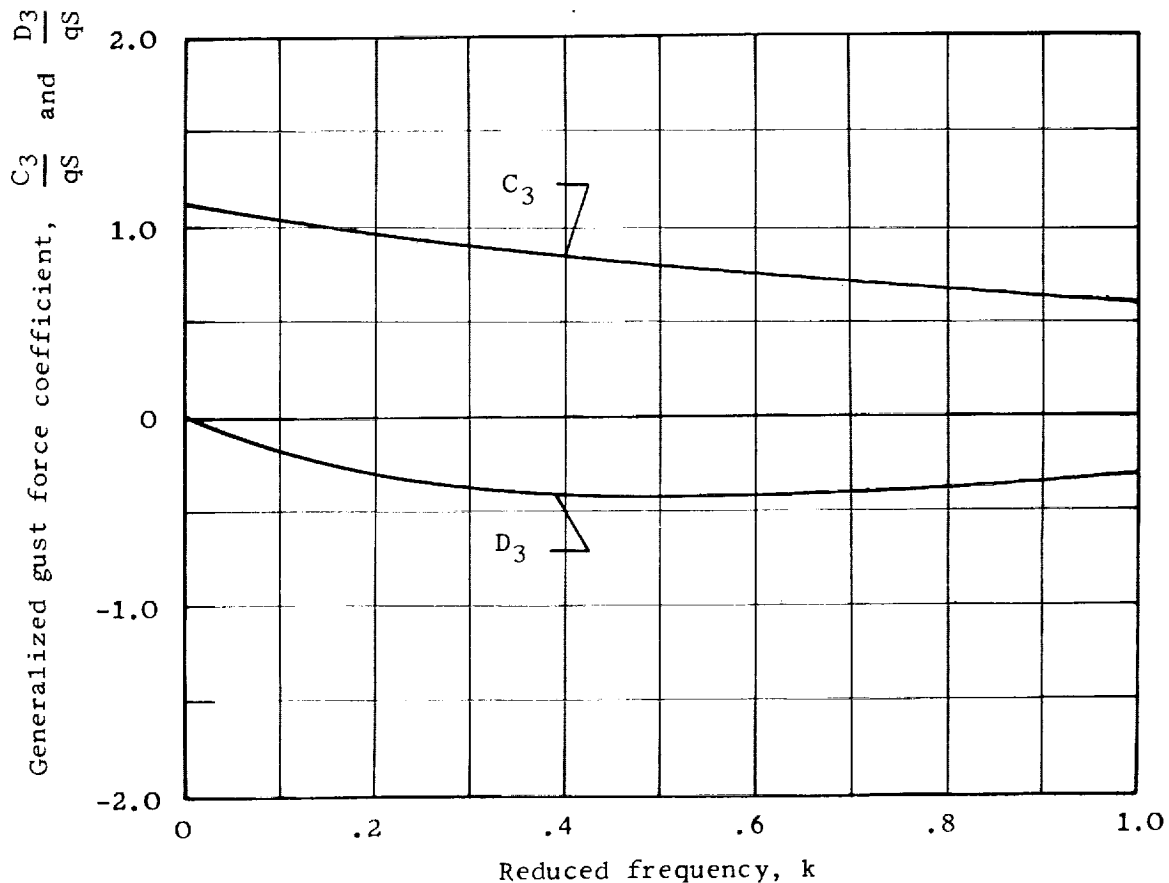
(2) 75° delta wing; $A = 1.072$; $\lambda_T = 0$; $M = 0.4$.

Figure 4. Continued.



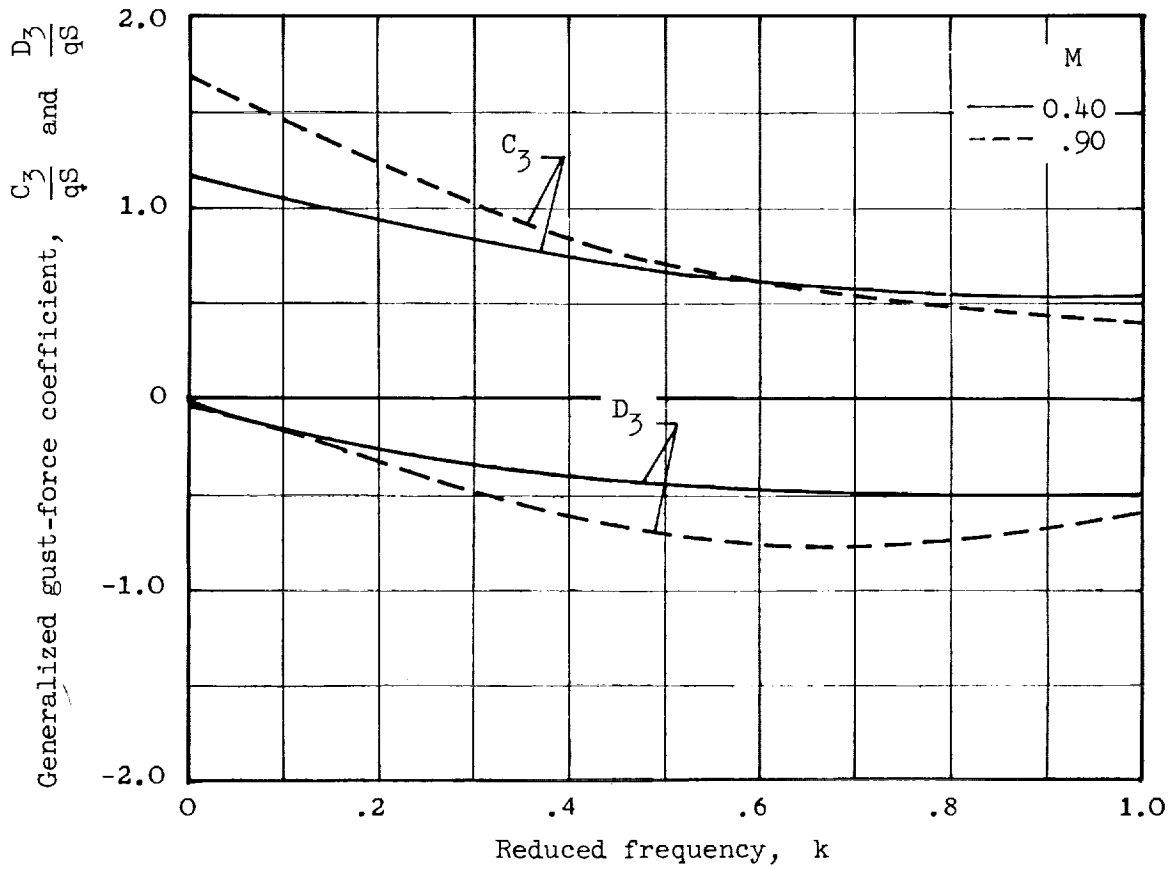
(m) 75° delta wing; $A = 1.072$; $\lambda_T = 0$; $M = 0.90$.

Figure 4.- Concluded.



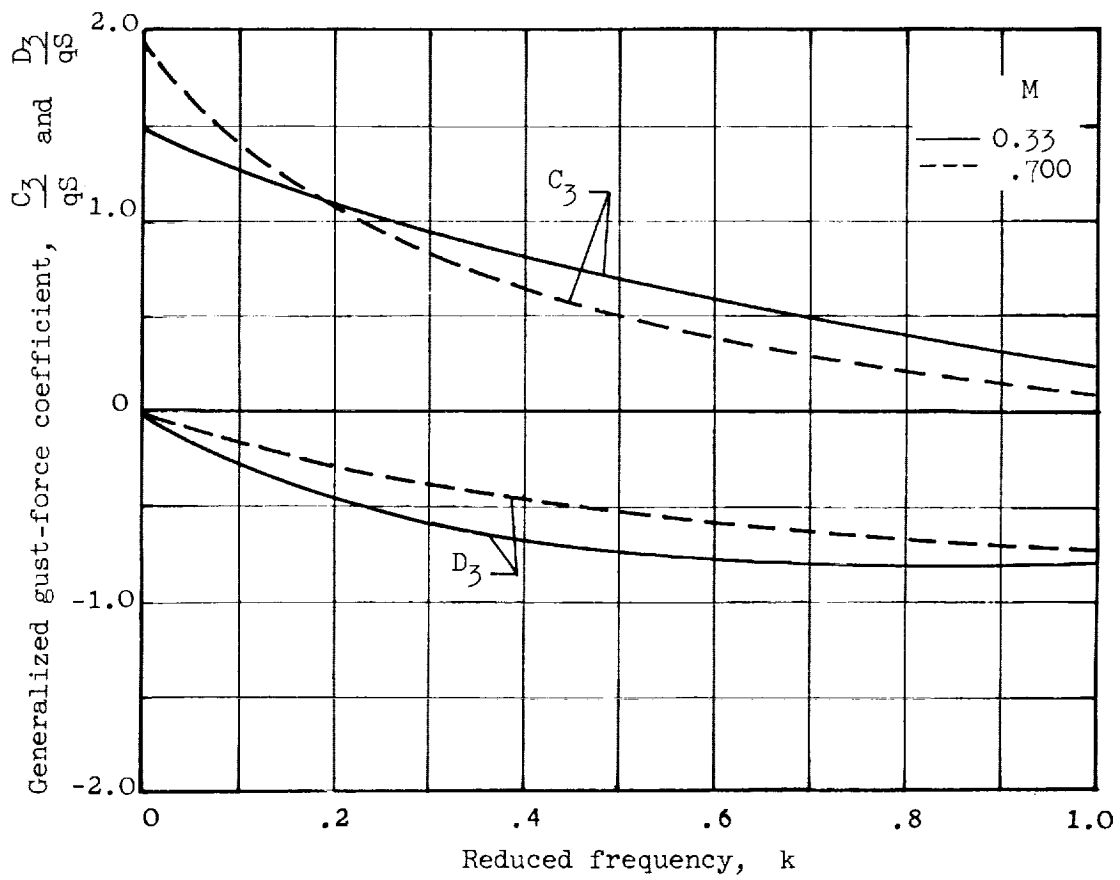
(a) Unswept wing; $A = 6.00$; $\lambda_T = 1.00$; $M = 0$.

Figure 5.- The variation with reduced frequency k of the in-phase and quadrature components of the generalized gust force for a wing deflection mode described by the parabola $z = (y^*)^2$. Generalized gust force is in coefficient form (i.e., divided by wing area and dynamic pressure) for a continuous sinusoidal gust field of unit velocity amplitude. The phase referral is to the gust velocity at the wing leading apex.



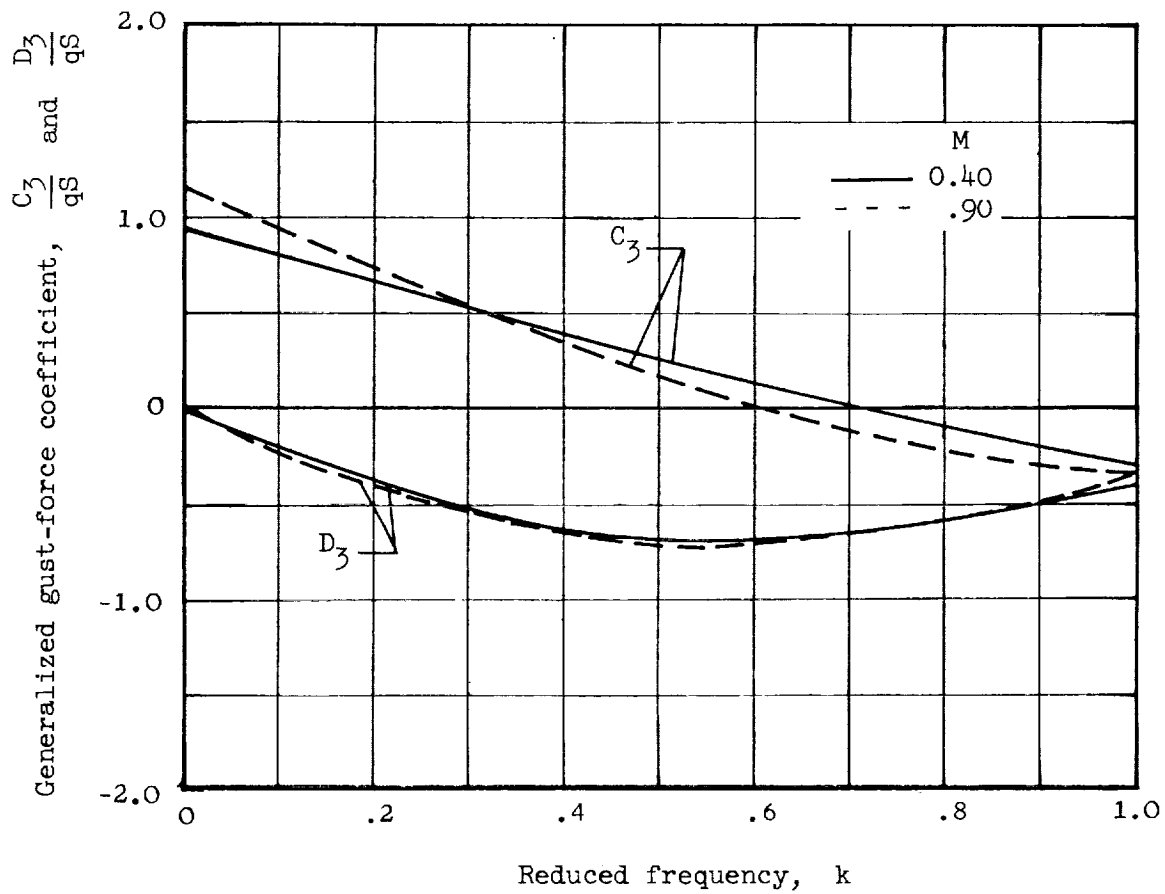
(b) Unswept wing; $A = 6.00$; $\lambda_T = 0.50$.

Figure 5.- Continued.



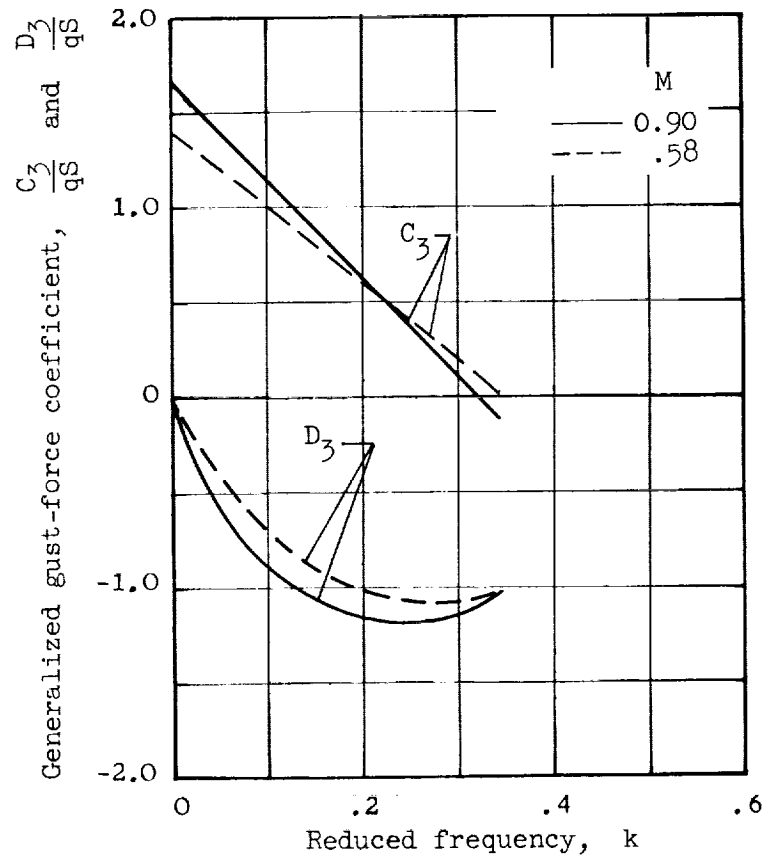
(c) 5° swept wing; $A = 11.60$; $\lambda_{T1} = 0.44$.

Figure 5.- Continued.



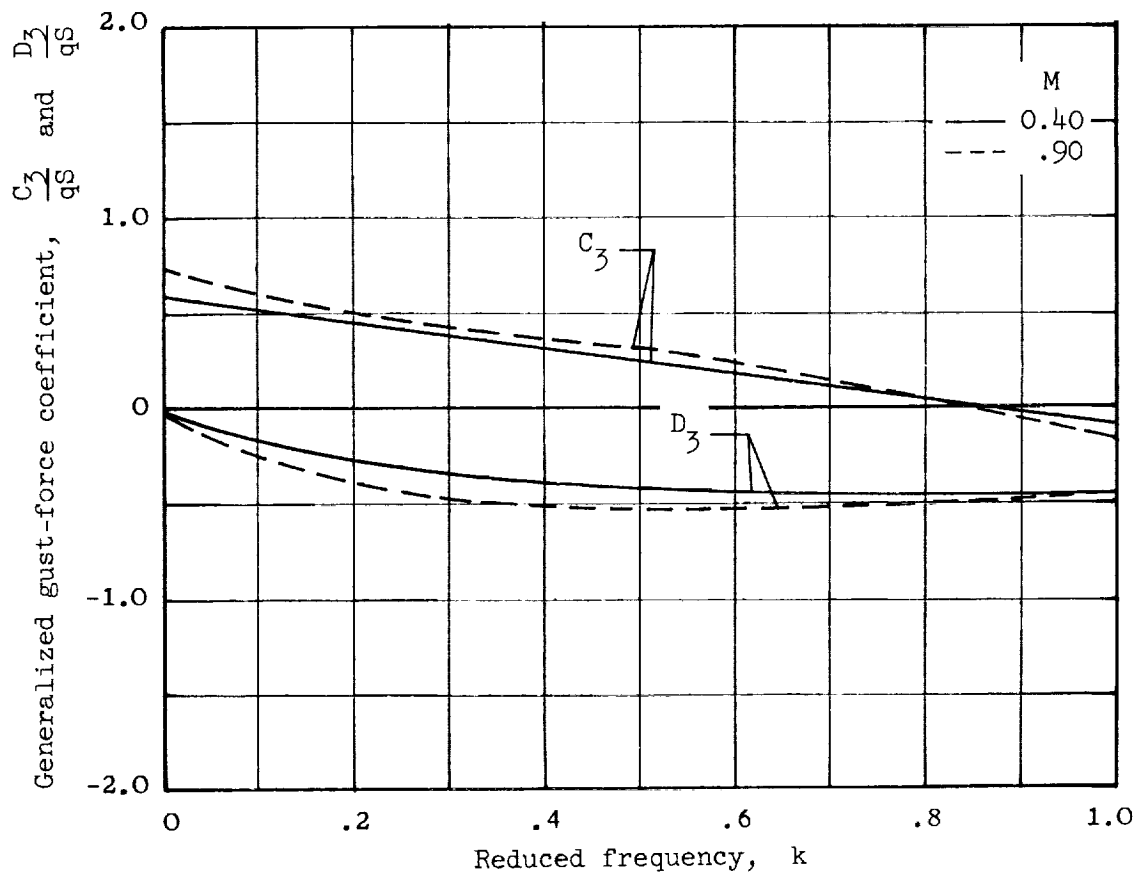
(d) 35° swept wing; $A = 4.00$; $\lambda_T = 0.42$.

Figure 5.- Continued.



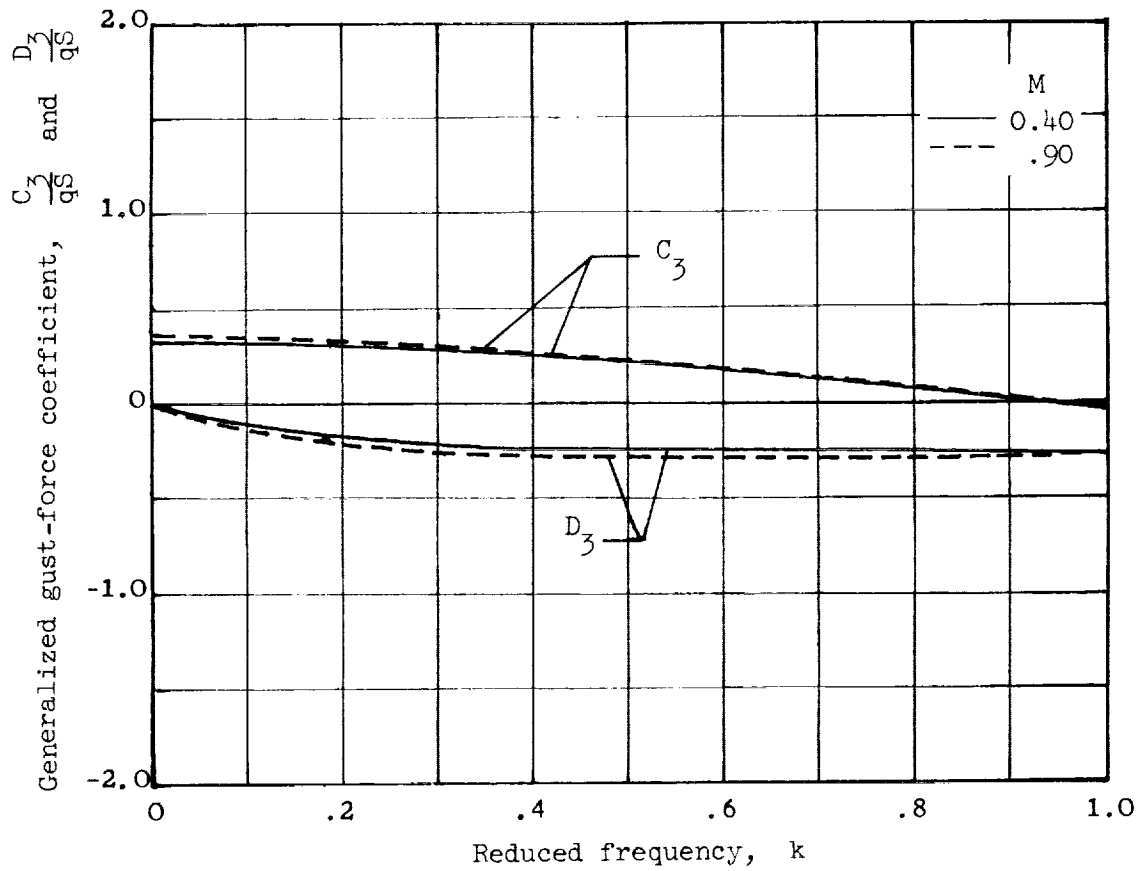
(e) 35° swept wing; $A = 9.43$; $\lambda_T = 0.42$.

Figure 5.- Continued.



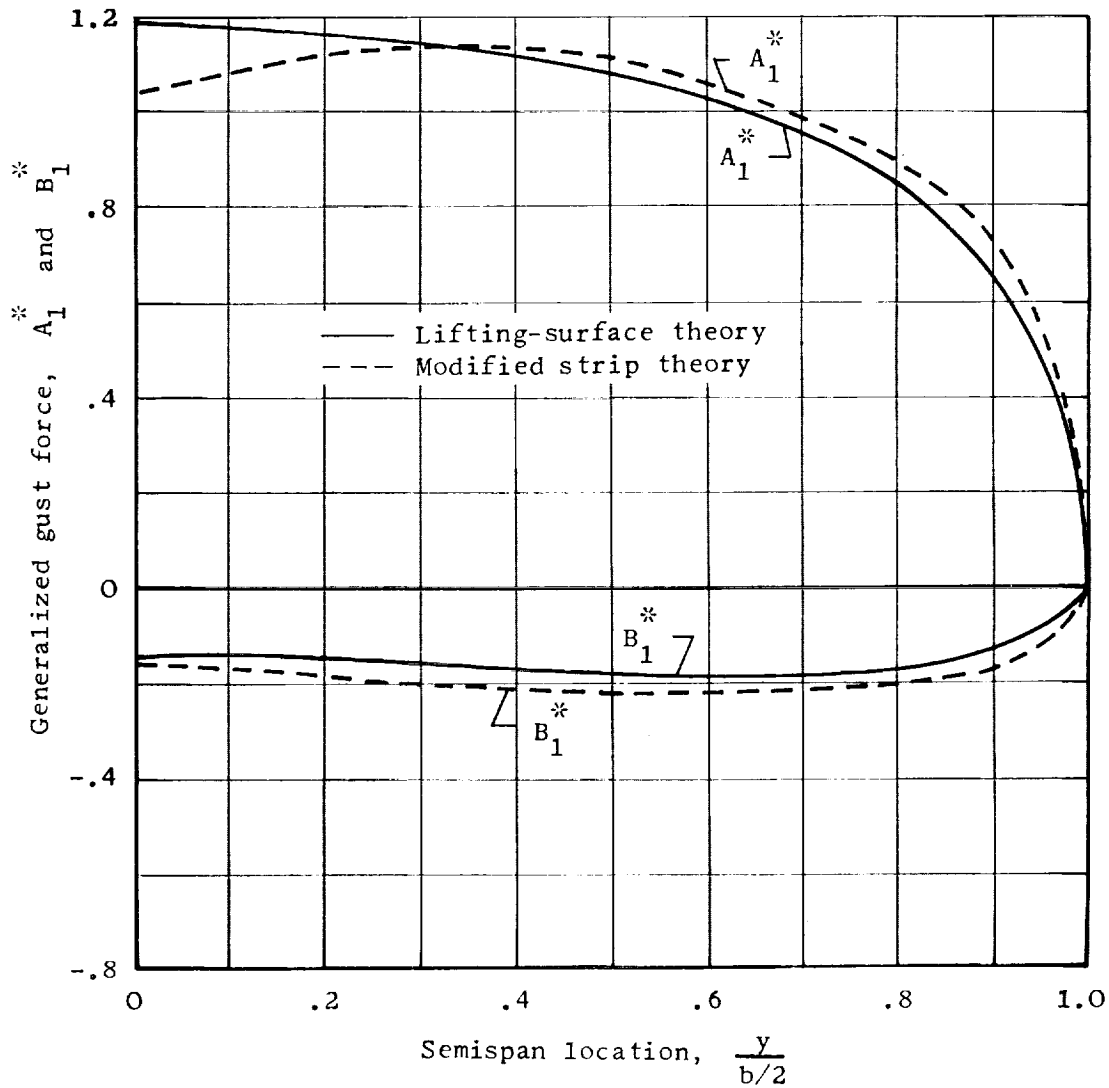
(f) 60° delta wing; $A = 2.30$; $\lambda_T = 0$.

Figure 5.- Continued.



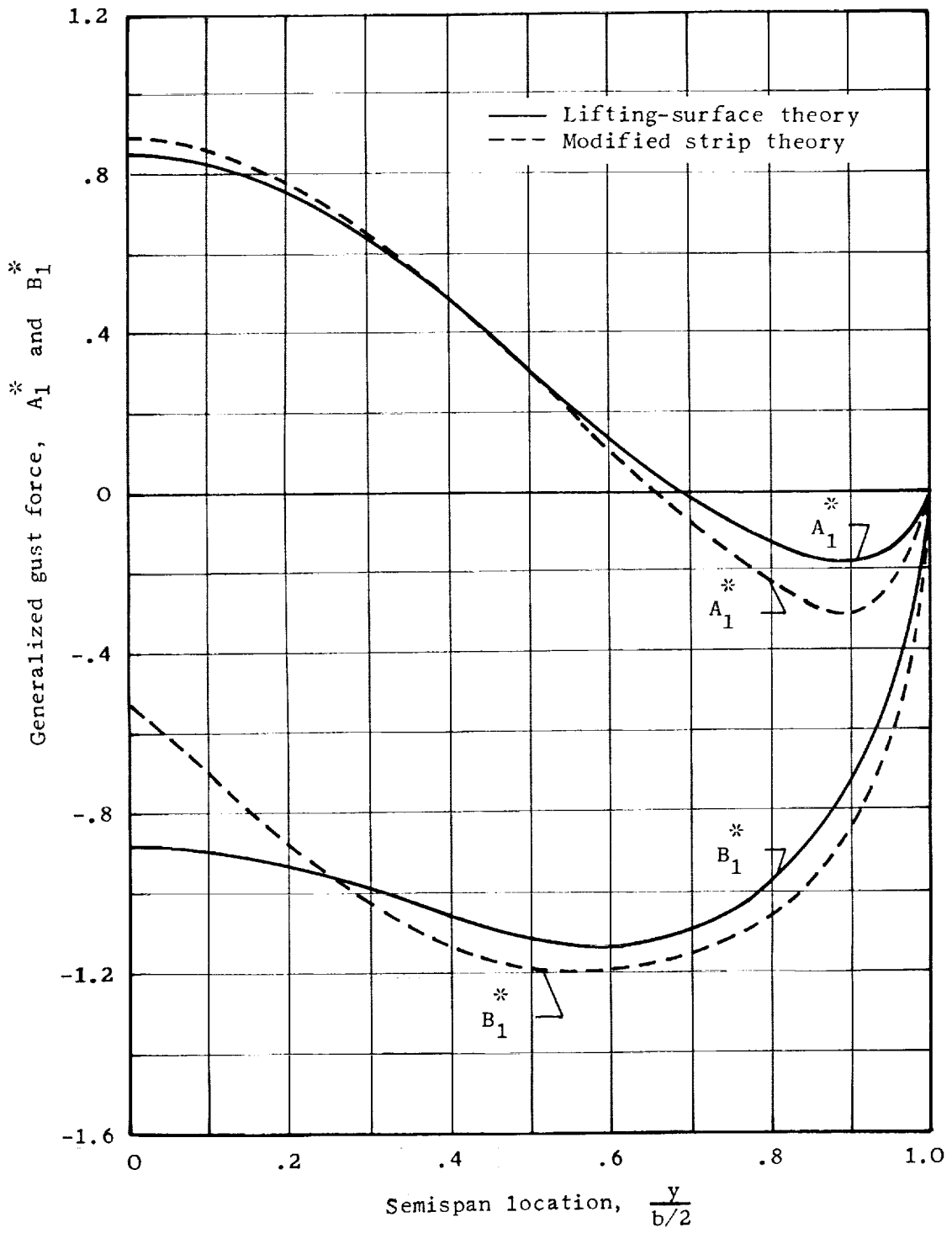
(g) 75° delta wing; $A = 1.07$; $\lambda_T = 0$.

Figure 5.- Concluded.



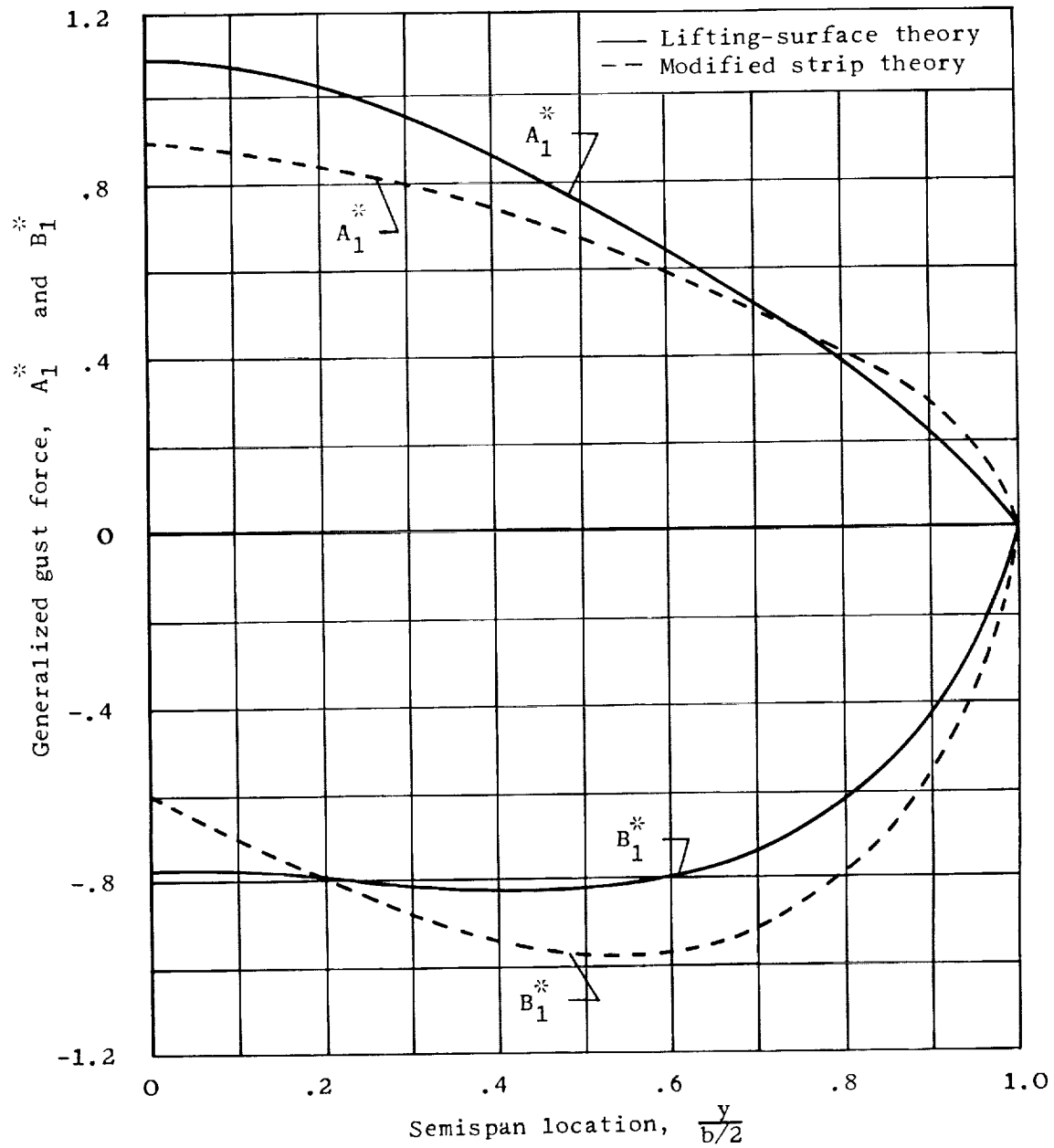
(a) 35° swept wing; $A = 9.43$; $\lambda_T = 0.42$; $M = 0.58$; $k = 0.034$.

Figure 6.- A comparison of results from lifting-surface theory and from modified strip theory for spanwise distributions of the in-phase and quadrature components of the generalized gust force tending to produce vertical translation (equivalent to section lift), normalized by division by the magnitude of the total lift $\sqrt{C_1^2 + D_1^2}$.



(b) 35° swept wing; $A = 9.43$; $\lambda_T = 0.42$; $M = 0.58$; $k = 0.343$.

Figure 6.- Continued.



(c) 60° delta wing; $A = 2.30$; $\lambda_T = 0$; $M = 0.40$; $k = 0.50$.

Figure 6.- Concluded.

